

AD-775 857

INCLUSION OF TIP RELIEF IN THE PREDICTION OF COMPRESSIBILITY EFFECTS ON HELICOPTER ROTOR PERFORMANCE

John M. LeNard, et al

Aerophysics Company

Prepared for:

Army Air Mobility Research and Development Laboratory

December 1973

DISTRIBUTED BY:

NTIS

National Technical Information Service
U. S. DEPARTMENT OF COMMERCE
5285 Port Royal Road, Springfield Va. 22151

AD

AD 75857

USAAMRDL TECHNICAL REPORT 73-71

**INCLUSION OF TIP RELIEF IN THE PREDICTION OF
COMPRESSIBILITY EFFECTS ON HELICOPTER ROTOR
PERFORMANCE**

By

John M. LeNard
Gabriel D. Boehler

December 1973

**EUSTIS DIRECTORATE
U. S. ARMY AIR MOBILITY RESEARCH AND DEVELOPMENT LABORATORY
FORT EUSTIS, VIRGINIA**

CONTRACT DAAJ02-72-C-0031
AEROPHYSICS COMPANY
WASHINGTON, D.C.

Approved for public release;
distribution unlimited.



Approved for public release;
distribution unlimited.

DDC
RECEIVED
MAR 20 1974
REGULATED
B

DISCLAIMERS

The findings in this report are not to be construed as an official Department of the Army position unless so designated by other authorized documents.

When Government drawings, specifications, or other data are used for any purpose other than in connection with a definitely related Government procurement operation, the United States Government thereby incurs no responsibility nor any obligation whatsoever; and the fact that the Government may have formulated, furnished, or in any way supplied the said drawings, specifications, or other data is not to be regarded by implication or otherwise as in any manner licensing the holder or any other person or corporation, or conveying any rights or permission, to manufacture, use, or sell any patented invention that may in any way be related thereto.

Trade names cited in this report do not constitute an official endorsement or approval of the use of such commercial hardware or software.

DISPOSITION INSTRUCTIONS

Destroy this report when no longer needed. Do not return it to the originator.

ACCESSION BY	
DDP	DDP: Section <input checked="" type="checkbox"/>
DDP	DDP: Office <input type="checkbox"/>
DDP: OFFICE	<input type="checkbox"/>
JUSTIFICATION	
BY	
DISTRIBUTION/AVAILABILITY CODES	
DDP	DDP: Sec/Spec <input type="checkbox"/>
A	

ia



DEPARTMENT OF THE ARMY
U S ARMY AIR MOBILITY RESEARCH & DEVELOPMENT LABORATORY
EUSTIS DIRECTORATE
FORT EUSTIS, VIRGINIA 23804

This report has been reviewed by the Eustis Directorate, U.S. Army Air Mobility Research and Development Laboratory and is considered to be technically sound.

The purpose of this effort was to develop the methods for applying the tip relief theory of USAAMRDL TR 72-7 to rotor performance analysis. The technique for predicting rotor compressibility power losses is discussed, and charts of calculated results illustrating power losses due to tip relief as functions of both advance ratio and tip Mach number are included. Computer programs for direct application of tip relief to rotor performance strip analysis and for the separate calculation of tip relief are included.

This program was conducted under the technical management of Mr. James F. Trant, Jr., of the Systems Support Division.

UNCLASSIFIED

Security Classification

DOCUMENT CONTROL DATA - R & D		
<i>(Security classification of title, body of abstract and indexing annotation must be entered when the overall report is classified)</i>		
1. ORIGINATING ACTIVITY (Corporate author) Aerophysics Company Washington, D.C.		2a. REPORT SECURITY CLASSIFICATION UNCLASSIFIED
		2b. GROUP
3. REPORT TITLE INCLUSION OF TIP RELIEF IN THE PREDICTION OF COMPRESSIBILITY EFFECTS ON HELICOPTER ROTOR PERFORMANCE		
4. DESCRIPTIVE NOTES (Type of report and inclusive dates) Final Report		
5. AUTHOR(S) (First name, middle initial, last name) John M. LeNard Gabriel D. Boehler		
6. REPORT DATE December 1973	7a. TOTAL NO. OF PAGES 60	7b. NO. OF REFS 53
8a. CONTRACT OR GRANT NO. DAAJ02-72-C-0031	8b. ORIGINATOR'S REPORT NUMBER(S) USAAMRDL TECHNICAL REPORT 73-71	
9. PROJECT NO. 1F1G2206A:61		
c.	9b. OTHER REPORT NO(S) (Any other numbers that may be assigned this report) Aerophysics Company Report AR-59	
d.		
10. DISTRIBUTION STATEMENT Approved for public release; distribution unlimited.		
11. SUPPLEMENTARY NOTES		12. SPONSORING MILITARY ACTIVITY EUSTIS DIRECTORATE U.S. Army Air Mobility Research and Development Laboratory Fort Eustis, Virginia
13. ABSTRACT The tip relief effect on the performance of helicopters operating at high subsonic tip Mach numbers is calculated. The theoretical method based on the complementary wing model for tip relief is applied. The method of application in complex blade element computer programs is described and results are presented. Similarly, the technique and results from a simplified application for use in energy type prediction methods are given. Since tip relief is closely connected with the problem of predicting the compressible power loss of rotors, the techniques for predicting this power loss are reviewed and discussed in detail.		

DD FORM 1473

REPLACES DD FORM 1473, 1 JAN 64, WHICH IS OBSOLETE FOR ARMY USE.

UNCLASSIFIED

Security Classification

12

63

UNCLASSIFIED
Security Classification

14. KEY WORDS	LINK A		LINK B		LINK C	
	ROLE	WT	ROLE	WT	ROLE	WT
Rotary wing						
Helicopter performance						
Three-dimensional flow						
Compressible flow						
Tip relief						
Wing theory						
Aspect ratio						

UNCLASSIFIED

Security Classification

10

13067-73

Project 1F162206AA61
Contract DAAJ02-72-C-0031
USAAMRDL Technical Report 73-71
December 1973

INCLUSION OF TIP RELIEF IN THE PREDICTION OF
COMPRESSIBILITY EFFECTS ON HELICOPTER ROTOR
PERFORMANCE

Final Report

Aerophysics Company Report AR-59

By

John M. LeNard
Gabriel D. Boehler

Prepared by

Aerophysics Company
Washington, D. C.

for

EUSTIS DIRECTORATE
U.S. ARMY AIR MOBILITY RESEARCH AND DEVELOPMENT LABORATORY
FORT EUSTIS, VIRGINIA

Approved for public release;
distribution unlimited.

ABSTRACT

The tip relief effect on the performance of helicopters operating at high subsonic tip Mach numbers is calculated. The theoretical method based on the complementary wing model for tip relief is applied. The method of application in complex blade element computer programs is described and results are presented. Similarly, the technique and results from a simplified application for use in energy type prediction methods are given. Since tip relief is closely connected with the problem of predicting the compressible power loss of rotors, the techniques for predicting this power loss are reviewed and discussed in detail.

FOREWORD

This investigation was sponsored by the Eustis Directorate, U.S. Army Air Mobility Research and Development Laboratory, under Contract DAAJ02-72-C-0031, Project 1F162206AA61, during the period December 1971 to February 1973.

The present work is a continuation of the work previously reported under USAAMRDL TR 72-7. The basic concept underlying the application of tip relief theory to rotary wings was suggested by Mr. James P. Trant, Jr., Eustis Directorate, USAAMRDL. Mr. Trant was the technical representative of the Contracting Officer for this contract. His continued assistance and guidance during the program are gratefully acknowledged. The material from a limited distribution paper was made available by the Douglas Aircraft Company, McDonnell Douglas Corporation.

TABLE OF CONTENTS

	<u>Page</u>
ABSTRACT.....	iii
FOREWORD.....	v
LIST OF ILLUSTRATIONS.....	viii
LIST OF SYMBOLS.....	ix
INTRODUCTION.....	1
COMPRESSIBILITY EFFECTS IN HELICOPTER AERODYNAMICS.....	2
Compressible Fluid Dynamics of Rotary Wings.....	2
Early Experimental Work.....	3
Blade Element Analysis.....	4
Empirical Methods.....	5
Analytical Calculation of the Compressibility Effects on Rotor Performance.....	6
TIP RELIEF IN ITS RELATIONSHIP TO COMPRESSIBILITY.....	10
Description of Theory.....	10
The Use of the Tip Relief Correction in Strip Analysis.....	14
A Simplified Blade Element Analysis To Calculate Tip Relief.....	16
Tip Relief Effect on Performance.....	21
Tip Relief Combined with Compressibility.....	26
Tip Relief Calculation as Proposed by Prouty.....	28
DISCUSSION OF SIMILARITY LAWS FOR ROTORS.....	31
COMMENTS ON EXPERIMENTAL VERIFICATION OF COMPRESSIBILITY EFFECTS AND TIP RELIEF.....	33
CONCLUSIONS AND RECOMMENDATIONS.....	35
LITERATURE CITED.....	36
APPENDIX. Computer Programs.....	41
DISTRIBUTION.....	50

LIST OF ILLUSTRATIONS

	<u>Page</u>
<u>Figure</u>	
1 Effects of Compressibility on Rotors in Hover.....	8
2 Complementary Wing and Coordinate System for a Finite Wing.....	11
3 Application of the Tip Relief Correction.....	15
4 Drag Distribution on a Hovering Rotor.....	17
5 Change in Torque Coefficient Due to Tip Relief.....	23
6 Change in Torque Coefficient Due to Tip Relief.....	24
7 Change in Torque Coefficient Due to Tip Relief, Some Comparisons.....	25
8 Typical Comparison of Test and Predicted Power Required...	26
9 Comparison of Compressibility Effects.....	28

LIST OF SYMBOLS

a	Speed of sound, ft/sec
a_c	Slope of C_D with M using a straight-line approximation
b	Number of blades
c	Semichord, ft
C_D	Drag coefficient
C_L	Lift coefficient
C_P	Pressure coefficient
C_F	Rotor power coefficient
C_Q	Rotor torque coefficient
C_{Qo}	Rotor profile drag torque coefficient
C_T	Rotor thrust coefficient
D	Drag, lb
D'	Distance, ft, = $\sqrt{(x-\xi)^2 + (y-\eta)^2 + z^2}$
F	z-coordinate of wing or blade surface, ft
\bar{G}_x	Correction factor, namely, equivalent fractional change in free-stream velocity, due to tip relief
G	Source potential of complementary wings, ft
h_n	Terms of the Taylor series expansion of \bar{G}_x , ft ⁻ⁿ
I_n	Geometric characteristic of airfoil, = $\int_c^{+c} F_\xi \xi^{(2(n-1)+1)} d\xi$, ft ²ⁿ
K	Constant for parabolic variation of C_D with M
α	Incompressible lift curve slope, per radian
M	Mach number
M'	Mach number at which drag increases from incompressible value for straight-line approximation
M_{dd}	Drag divergence Mach number
M_{ld}	Lift divergence Mach number

R	Total radius of a blade, ft
r	Radial station, ft
\bar{r}	Nondimensional radial station, = r/R
u	Local velocity, ft/sec
U_∞	Free-stream velocity, ft/sec
V	Forward speed, ft/sec
x,y,z	Coordinate system (see Figure 2), ft
α	Angle of attack, radians
β	Prandtl-Glauert factor, $\sqrt{1-M^2}$
γ	Ratio of specific heats
Γ	Stagnation compressibility factor; $1 + \frac{\gamma-1}{2} M^2$
λ	Aspect ratio
μ	Advance ratio
ρ	Density, slugs/ft ³
ξ, η, ζ	Auxiliary coordinates (see Figure 2), ft
σ	Solidity
τ	Thickness ratio
ϕ	Potential function, ft ² /sec
ψ	Azimuthal angle, deg
Ω	Rotational speed, rad/sec

SUPERSCRIPTS

$(\bar{\quad})$	Averaged
$(\tilde{\quad})$	Reduced value in accordance with the transonic similarity rules

SUBSCRIPTS

$()_c$	Compressible
$()_{eff}$	Effective
$()_{FW}$	Finite wing
$()_i$	Induced
$()_{inc}$	Incompressible
$()_m$	Maximum
$()_o$	Due to profile drag
$()_{TR}$	Due to tip relief
$()_x$	Differentiation with respect to x
$()_y$	Refers to local value
$()_\infty$	Condition in the undisturbed stream
$()_\xi$	Differentiation with respect to the auxiliary variable
$()_{1,90}$	Refers to value at $\bar{r}=1$, and $\psi=90^\circ$ on an advancing rotor
$()_1$	Refers to value at $\bar{r}=1$ on a hovering rotor

NOTATION

$A(B)$	A is a function whose variable is B
Δ	Incremental value of following quantity
d	Derivative operator
∂	Partial derivative operator
\int	Integral operator
Σ	Summation
$()_i$ or $()_{i,j}$	Element in a summation

INTRODUCTION

Compressibility effects have long been recognized as having an important influence on the performance of high-speed helicopters. During the 1960's, it gradually became recognized that one could "live with" compressibility effects on rotors. Earlier it was found, first on propellers and then on rotors, that adverse effects of compressibility occurred at higher Mach numbers than expected from fixed-wing results. The next obvious step was to attempt to alleviate compressibility effects through such techniques as the use of thinner or supercritical airfoils near the tip of the blade, shaping of the tip, etc. Parallel efforts were directed at developing techniques for predicting performance of rotors considering compressibility and correlating flight test data. Further studies and experimentation are continuing at a fast pace.

This report presents the results of an investigation conducted by Aerophysics Company to obtain a better theoretical understanding of compressibility effects on helicopter rotor performance. It exploits earlier findings by LeNard¹ based on a hypothesis suggested by Trant that a theoretical potential flow method of source - sink singularities similar to the method developed by Anderson for fixed wings² could account for the effect of the compressible three-dimensional relief on the torque required for a helicopter rotor. Results of Reference 1 were systematically analyzed in the study reported herein for application with existing rotor performance analyses. Since the main point of the study is tip relief, i.e., a relief effect not accounted for in conventionally-used compressibility calculations, it was necessary to carefully review these conventional compressibility analyses. These analyses are summarized in the first part of the report. Then, a brief review of the tip relief analysis of Reference 1 is presented. This tip relief analysis is then applied and used with existing blade element computer programs, both hover and forward flight, and in a very simplified blade element analysis whereby the torque decrease due to tip relief is calculated as a separate component of the total torque. Numerical examples are calculated and performance charts of the tip relief effect, usable for design purposes, are drawn.

As some of today's helicopter rotors encounter fully transonic flows, the transonic similarity rules derived for fixed wings were examined. It was hoped that these similarity laws could be extended to rotors and combined with the tip relief theory. Although this subject was examined and is discussed in this report, it has not yet been successfully applied to rotors.

Experimental verification of the Anderson - LeNard theory for tip relief of rotors has been considered; however, no simple and relatively inexpensive method has been suggested that will effectively isolate the tip relief effect to the precision required to verify the theory.

It is concluded that the Anderson - LeNard tip relief method has been successfully reduced to practice. Attention should now be concentrated on the other aspects of helicopter rotor compressibility.

COMPRESSIBILITY EFFECTS IN HELICOPTER AERODYNAMICS

The problems of high-speed rotors and propellers have been under investigation since the early 1940's. Propeller compressibility problems became acute on high-speed fighters during World War II. A number of approaches to subsonic and supersonic propeller performance evolved. During this period, experiments showed a discrepancy between the test results and blade element theory, in that the tests gave an apparently lower drag divergence Mach number. Many investigators have attempted to find means of predicting the compressible flow effects as are discussed here.

At high forward speeds it is difficult to separate compressibility and stall effects, as both often occur at the same time on the rotor. At the advancing tip, the forward speed and the rotational speeds add, resulting in speeds approaching Mach one. But on the retreating side the two speeds subtract, resulting in a region of reverse flow and areas where the flapping blades are at or above the stall angle of attack. The dividing line between stall losses and compressibility losses is seldom deducible from test data, and both areas must be taken into account in rotor analysis.

COMPRESSIBLE FLUID DYNAMICS OF ROTARY WINGS

The motion of rotating wings through a fluid should be describable by the basic differential equations of fluid motion. But the complexity of the rotary-wing problem is such that only recently has any real progress been made in the basic theory. The fluid dynamic equations governing the motion of the fluid for a rotating wing can be derived from the equations of continuity, momentum and energy. This derivation is presented in a number of places.^{1,3,4,5,6}

Sears⁷ made one of the first attempts at beginning rotary-wing theory with the basic governing equations of fluid motion in 1950. He investigated the flow potential function of an infinitely long cylindrical blade, rotating in incompressible flow. The result indicated that the potential per unit velocity in the plane transverse to the rotating cylinder is the same as for a similar cylinder in steady plane flow. Further, immediately adjacent to the cylinder (at least for the circular cylinder case given in Sears' paper) the flow is only in this transverse plane. The conclusion which may be drawn is that the pressure coefficient and therefore the force coefficients from potential, incompressible flow are the same as that from blade element theory. Thus the validity of the blade element approach was indicated, and it has been used for performance calculations and theoretical work including turbulent, compressible rotor boundary layers (for example, see Hicks and Nash,⁸ or Clark and Arnoldi,⁹). Only in December 1970 was it shown by Goorjian and McCroskey¹⁰ that the Sears approach is not necessarily valid when the rotating blade is of finite span. The major theoretical effort over the past 15 years has been toward determining the effect of the trailing vortices. The trailing vortices give the local inflow velocity, which is a major quantity in determining the local angle of attack, particularly near the tip and in hover. A great amount of literature is available on this approach^{11,12}

and thus will not be discussed in detail here, but it generally considers incompressible flows.

In the case of uniform flows, the well-known Prandtl-Glauert transformation may be used to change the equation for small perturbation velocities in compressible flows to the equation for an equivalent incompressible flow. It was shown in Reference 5 that small perturbation equations for a rotating blade do not reduce to a simple form, amenable to the Prandtl-Glauert transformation. Further assumptions are needed so that a Prandtl-Glauert type of transformation may be used, as shown in Reference 1. The difference between the two cases is that for uniform flow the compressible, small-perturbation equation has constant coefficients, while in rotating flow it is again a linear, second-order partial differential equation, but the coefficients are now functions of the space variables.

There have been two recent papers concerning the compressible potential flow over nonlifting, hovering rotor blades. The earlier one by Sopher⁵ derives the equation for a source distribution representing a thin airfoil, rotating blade of finite span in the subsonic, compressible regime. The inviscid velocity distribution was then calculated at several spanwise stations. Results from numerical solutions to the equations for transonic flow over a rotating blade were presented by Caradonna and Isom.⁶ This paper indicated that as the Mach number increases, "the nonlinear behavior of the wing near the tip becomes more severe than that of the rotor". Thus linearized theory (subsonic flow) has validity to higher subsonic Mach numbers for a rotor than for a wing.

The asymptotic expansion to the linearized subsonic potential equation in terms of the distance from the tip was derived by Caradonna and Isom.⁶ To a first approximation near the tip, the flow was found to be the same as the three-dimensional flow in the tip region of a semi-infinite wing moving at a uniform speed equal to the blade tip Mach number. This is valid for high-aspect-ratio rotors where the Mach number gradient is large. But in the high-subsonic compressible range, small changes in the Mach number can result in large changes in the drag. Thus this approximation must be used with care.

EARLY EXPERIMENTAL WORK

Although some experimental work was done during the 1940's, by Gutsche¹³ and Gustafson¹⁴ among others, the major work in this area is the result of a series of tests conducted on the NACA Langley test tower under the direction of Paul Carpenter.

The Carpenter tests were performed on a number of different rotors, varying blade airfoil section. Reports of these tests are given in references 15 through 25. Comparison of the test results^{16,20} with strip analysis of Reference 26 using two-dimensional airfoil data indicated that the theory overestimated the compressibility drag rise. Carpenter²¹ gave as reasons for these discrepancies the effect of centrifugal pumping and the drag-alleviating effects of three-dimensional flow at the blade tip resulting from a reduction of local Mach number. This led him to formulate the concept of synthesized blade section data.

Synthesized data is obtained by adjusting the airfoil section properties until the strip analysis performance prediction agrees with the measured performance. This is a trial and error approach, but certain guidelines from theory and test are used to obtain reasonable values of the airfoil section properties.²¹

The synthesized data is obtained from hover tests on a test tower. Reasonably large blades (26.8 feet radius and 16.4 inches chord for the NACA 0012 airfoil, for example) were used, to obtain high enough Reynolds numbers, but surface condition differences may be important. Concerning application to forward flight, Carpenter states that the synthesized data should be valid until proved otherwise.²¹ To date this hypothesis has been neither proved nor disproved.

One of the possible applications envisioned for the tip relief theory is to provide a link between synthesized airfoil data and two-dimensional airfoil data. The synthesized airfoil data is, in a sense, an average of the two-dimensional data with tip relief correction.

BLADE ELEMENT ANALYSIS

Blade element or strip analysis forms the basis of almost all performance and rotor dynamics calculations. The so-called "energy" methods are in most instances the result of simplifying the strip analysis so that the integration may be carried out analytically (i.e., resulting in an algebraic equation), rather than requiring numerical computation.

The basis of blade element theory is the assumption that each element can be considered aerodynamically as an independent two-dimensional airfoil segment. The local forces are calculated from the resultant velocities at the element, and the total forces are found by integrating radially and azimuthally. From the forces, the motion of the element is determined. But the motion (especially flapping) has an effect on the local velocities and therefore the forces, requiring iterations.

The early performance methods made a number of assumptions to avoid the iterative calculations. These concerned the induced velocities, the lift and drag coefficients, the flapping motion, etc. An example may be found in Chapter 8 of the book by Gessow and Myers,²⁷ although other workers have used different sets of assumptions.

With the development of computers, an iterative method is used, which in essence was first outlined by Gessow.²⁶ There have been a number of improvements made in various areas since that time. The most widely used results of this technique are the tables and charts prepared by Tanner.^{28,29}

There is much work still being done and controversy over the airfoil data to be used for these computerized strip analyses. The latest suggestions concern the problem of unsteady stall hysteresis.³⁰ The Tanner charts²⁸ use airfoil data from "two-dimensional wind tunnel tests of a production

blade specimen using the NACA 0012 airfoil section". A similar set of charts was prepared using the Carpenter²¹ synthesized data by Kisielowski et al.³¹ To our knowledge there has been no meaningful comparison of these two prediction methods, although both appear to be widely used.

The method proposed to account for tip relief is to use the two-dimensional airfoil data, but to make the corrections as indicated by the Anderson - LeNard theory. Detailed derivation of the tip relief theory is given in Reference 1, while the technique in general and the results of use in strip analysis are described in the following chapter.

To obtain an indication of the compressible power loss, Gessov and Crim³², using compressible airfoil data in the method described in Reference 26, calculated the power required for several rotor configurations. The compressible profile power loss of the various configurations was compared at equal values of the increment in tip Mach number above the drag divergence Mach number. The results showed that the different configurations had approximately the same loss in profile power coefficient to solidity ratio when compared in this manner. This suggested that the increment in power coefficient to solidity ratio due to compressibility depends only on the difference between the drag divergence and the advancing tip Mach numbers. A more detailed discussion is given later in this report in reference to Figure 9.

EMPIRICAL METHODS

To reduce the data and decrease the amount of flight test required, personnel at the Edwards AFB Flight Test Center have been developing an approach, mainly empirical, to account for compressibility effects. Drawing on fixed-wing experience, the power required is divided into two portions: (1) the incompressible power and (2) an increment in power due to compressible flow, which depends on the difference between the critical Mach number of the blade section and the Mach number of the element. The correlation is established empirically using UH-1F, CH-47A and CH-3E flight test data.^{33,34} References 35, 36, and 37 give detailed flight test data for these helicopters flying in the compressible flow regime. Later reports^{38,39} include the effects of power losses due to retreating blade stall.

The early empirical work^{33,34} attempted to relate the power increase due to compressibility to the value of the advancing tip Mach number above the critical Mach number. These works differ from Reference 32, where the drag divergence Mach number is used instead. Good correlation using test data from two different helicopters has been reported.³⁴ The resulting empirical relation for the compressible power rise has been used with varying success at Edwards and elsewhere.

More recently, a number of analytical/semiempirical techniques were developed and evaluated.^{38,39} These techniques used various approximations for the drag in compressible flow and the lift in the stall region. Thus both the compressibility and the stall regions are considered. The basic theory was modified empirically to obtain better correlation with data.

The techniques consider a number of variables, including lift coefficient at the advancing and retreating tip, lift curve slope as a function of Mach number, an empirical critical Mach number, maximum lift coefficient, Mach number distribution over the areas affected by compressibility and stall, and the calculation of these areas. Results are compared to the CH-3C flight test data in Reference 39. Since this report is widely available, and a number of techniques are presented, we will not discuss it in detail. Somsel³⁹ obtains correlation within $\pm 1 \times 10^{-5}$ in power coefficient over 80% of the flight envelope. But the remaining 20% occurs at the higher advance ratios, thrusts and Mach numbers.

ANALYTICAL CALCULATION OF THE COMPRESSIBILITY EFFECTS ON ROTOR PERFORMANCE

By analytical calculation we mean those approaches which attempt to yield an algebraic expression for the forces on a rotor due to compressibility and thus separate the forces due to compressibility from the other components of the total force. This falls into the realm of "energy" type approaches. These analytical calculations use one of two methods: actuator disc theory or blade element analysis.

In the late 1940's and early 1950's, the problem of high-speed propellers was investigated using actuator disc theory in compressible flow.^{40,41,42} In these investigations, the compressible flow through a contracting stream tube with energy added at the actuator disc is considered. This flow model represents axial flight and is more applicable to axial turbines and propellers at high forward speeds. The problem of compressible tip speed does not appear in the results due to the infinite number of blade assumptions inherent in the actuator disc approach. This actuator disc approach was combined with blade element theory by Laitone⁴³ for application to helicopters.

An approach which appears to be more applicable and useful was developed by Head,⁴⁴ by the use of theoretical and empirical rules for the variation of the drag and lift coefficients with Mach number. These variations are used in the blade element equations, which are then integrated to find the rotor thrust and torque coefficient ratios (i.e., the ratio of compressible to incompressible coefficients). Further, Head considers the increase due to compressibility in induced power, which is not done elsewhere.

Head's⁴⁴ paper may be outlined as follows: First, Head hypothesizes a variation of lift coefficient with Mach number. This variation was then used in the equations for torque and thrust for the hover case, which was then solved. He then examined the forward flight case. The compressible profile drag power, for both hover and forward flight, was then considered, hypothesizing a variation of drag coefficient with Mach number. This outline is followed in the discussion below.

The lift coefficient is assumed by Head to vary in accordance with the Prandtl-Glauert law for Mach numbers up to lift divergence. Above lift divergence, a linear decrease with Mach number is assumed.

$$C_L = \frac{m_0}{\delta} \quad M \leq M_{Ld} \quad (1)$$

$$C_L = \frac{m_0}{\delta} + \frac{d^2 L}{dM^2} (M - M_{Ld}) \quad M > M_{Ld} \quad (2)$$

Making the usual assumptions, such as small inflow angles, neglecting the effects of drag on the thrust and induced torque, etc., the compressible to incompressible ratio of thrust and induced torque coefficients are calculated for the hover case. These ratios are functions of the tip angle of attack, lift divergence and rotational Mach numbers, and the variation of lift coefficient with angle of attack and Mach number.

For the hover case, it is found that not only the torque but the thrust increases with Mach number. Thus most of the increased induced torque due to compressibility is due to the increase in thrust due to compressibility. Thus, given a required thrust, one would reduce the angle of attack (actually collective pitch) to make C_{Tc}/C_{Tinc} equal to unity. With this condition, the increase in induced torque due to compressibility does not exceed 3% at M_{Ld} and decreases above the lift divergence Mach number, since there is a relieving effect on lift that results in the inboard movement of the centroid of the load. These results from Reference 44 are shown in Figure 1. Parts (a) and (b) of Figure 1 show the effect of compressibility on thrust and angle of attack. In part (c), it can be seen that the induced torque due to compressibility at constant thrust is very small and may be neglected, while at a constant angle of attack this is not the case.

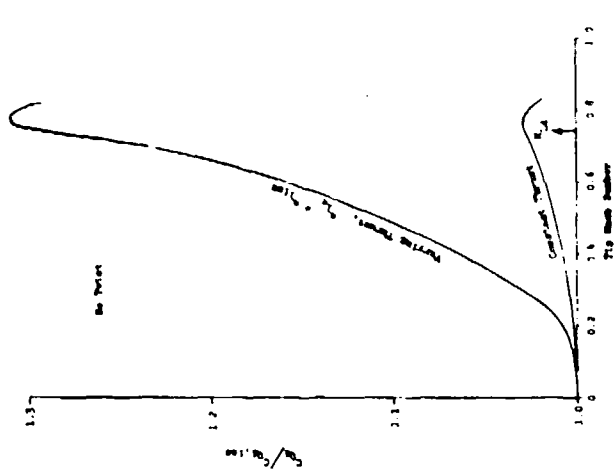
These results indicate that in hover, calculating only the incompressible values of the thrust and induced torque is a reasonable assumption in the usual energy calculations. The major effect of compressible flow on rotor performance is upon the profile power and upon the airfoil angle of attack. Much of the other work, as described herein, has been concerned with the profile power due to compressibility. On the other hand, the effect of compressibility on the angle of attack has been neglected.

For forward flight, Head states that the effect of compressibility on the induced power may be neglected and that the equation for thrust cannot be analytically integrated but must be numerically integrated, which he does not do.

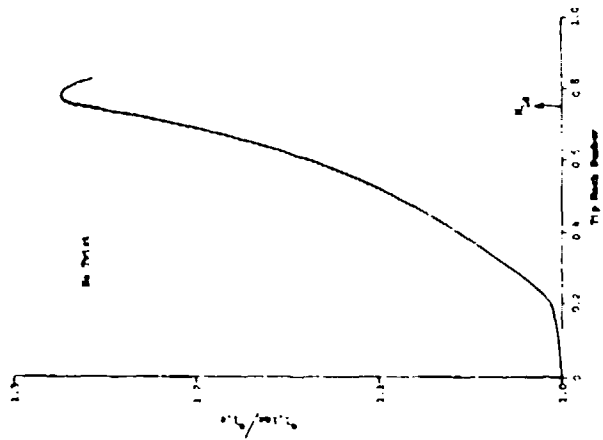
The calculation of compressible profile drag power is based on the assumption that the section drag coefficient variation with Mach number may be represented by a parabola. Head writes

$$\Delta C_{Q_{oc}} = \frac{\sigma}{4\pi} \int_{\psi} \int_{\bar{r}} (\mu \cos \psi + \bar{r})^3 \Delta C_D \bar{d}\bar{r} \, d\psi \quad (3)$$

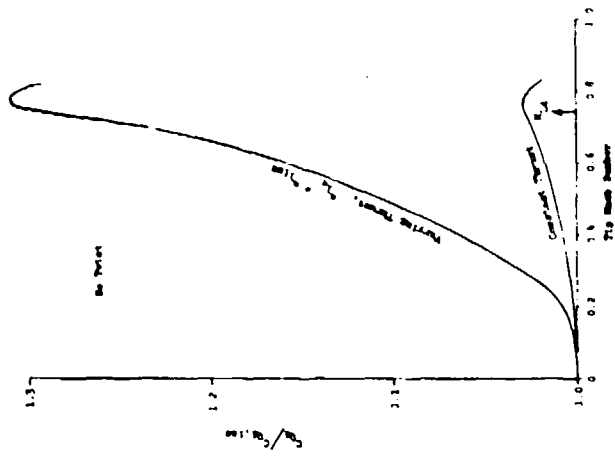
where the limits of integration on ψ and \bar{r} are chosen to represent the "portion of the rotor disc operating above the drag divergence Mach



(a) Thrust Coefficient at Constant Collective Pitch



(b) Angle of Attack at Constant Thrust Coefficient



(c) Induced Torque Coefficient

Figure 1. Effects of Compressibility on Rotors in Hover.⁴⁴

number" The incremental drag, ΔC_D , is the increase in profile drag due to compressibility. Head assumes basically a parabolic variation of ΔC_D with Mach number, but makes further correction, such as an increase of 0.06 for the rotor drag divergence Mach number above the two-dimensional value, quoting Reference 14. He carries out the integration indicated in equation (3) for both hover and forward flight. The results are presented in chart form, and $\Delta C_{Q_{OC}}$ may be calculated given $M_{1,90}$, μ , M_{dd} and the parameters for the parabolic variation of ΔC_D vs. M .

Results for hover appear very good when the Carpenter¹⁵ data is compared to the theory.⁴⁴ In forward flight, some limited comparison made to the data of Reference 35 appears to give low values of the ΔC_{Q_0} , but this result should not be taken as conclusive.

Further work with this theory is necessary to determine the importance of the change in angle of attack due to compressibility, the change in induced torque in forward flight due to compressibility, and comparisons to test data.

TIP RELIEF IN ITS RELATIONSHIP TO COMPRESSIBILITY

The existence of a tip relief effect has been suggested by various sources, as discussed in the previous chapter. The tip relief effect is a difference between the real three-dimensional flow over a finite span wing or rotor blade and the calculation for this wing or rotor blade made using two-dimensional airfoil data. In this chapter the theory and results from one approach to calculating the magnitude of the tip relief are given. The equations of the theory were derived in detail in Reference 1. Here the basic elements of the theory for its use are given and the results from its application in several performance calculations.

DESCRIPTION OF THEORY

For fixed-wing aerodynamics, the major effect of aspect ratio occurs in the spanwise variation of induced velocity and the resulting induced drag and angle of attack. This is all due to the production of lift by the finite fixed wing. At lower Mach numbers this approach is satisfactory, but at higher subsonic Mach numbers a further correction is needed, as was described by Anderson.²

When a three-dimensional object, such as a wing, is placed in a uniform flow, the stream lines around the body may deviate from the free stream in both directions perpendicular to the wing chord line. For a similar two-dimensional wing, only deviation in the direction perpendicular to the plane including both the chord and the span is possible. Thus one can qualitatively conclude that streamwise disturbances produced by three-dimensional bodies are lower in magnitude than those produced by two-dimensional wings. In the case of a rectangular planform wing of high aspect ratio, at the midspan the disturbances are nearly the same as for two-dimensional flow and diminish as the tip is approached, hence the name tip relief.

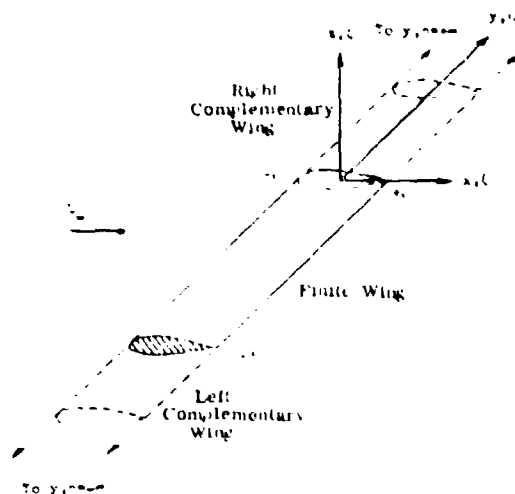
This qualitative concept was quantified for fixed wings by Anderson² through the use of linearized wing theory and the complementary wing concept. He showed that the difference between the two- and three-dimensional characteristic of a wing can, by proper averaging, be represented by a change from the actual free-stream velocity to an effective free-stream velocity. This will result in a change (decrease) of the effective Mach number and the dynamic pressure, hence in the drag coefficient.

Linearized wing theory represents the thickness by a source-sink distribution and the camber and angle of attack by a vortex distribution. The former gives the so-called nonlifting case, while the vortex distribution gives the lift. In a qualitative sense, we have shown that tip relief is due to displacement; hence we need consider only the thickness as given by the source-sink distribution.

The velocity induced due to thickness of a finite wing is the integral, over the planform, of a source-sink distribution determined by the local chordwise airfoil slope. The potential function of this wing is

$$\phi = U_{\infty}x - \frac{i}{2\pi} \int_{\text{Planform}} \frac{U_{\infty} F_{\xi}(\xi) d\xi d\eta}{D'} \quad (4)$$

$$\text{where } D'^2 = (x-\xi)^2 + (y-\eta)^2 + z^2 \quad (5)$$



This same potential function will result if this finite span wing is represented by a wing of infinite span less "complementary wings". The complementary wing is a similar wing extending from the tips of the finite wing to infinity on both sides. In the equation above the limits of the integral, using the coordinate system of Figure 2, is $+c$ and $-c$ on ξ , and -2λ and 0 on η . In the complementary wing representation the potential is

Figure 2. Complementary Wing and Coordinate System for a Finite Wing.

$$\begin{aligned} \phi = U_{\infty}x - \frac{1}{2\pi} \int_{-\infty}^{+\infty} \int_{-c}^{+c} \frac{U_{\infty} F_{\xi} d\xi d\eta}{D'} + \frac{1}{2\pi} \int_{-\infty}^{-2\lambda} \int_{-c}^{+c} \frac{U_{\infty} F_{\xi} d\xi d\eta}{D'} \\ + \frac{1}{2\pi} \int_0^{+\infty} \int_{-c}^{+c} \frac{U_{\infty} F_{\xi} d\xi d\eta}{D'} \end{aligned} \quad (6)$$

The first integral is identically the potential of an infinite or two-dimensional airfoil, and can be represented by the symbol $\phi_{\lambda=\infty}$. The last two integrals give values which vary with position throughout the flow field. Let $-G(\lambda, x, y, z)/U_{\infty}$ represent the third and fourth terms of equation (6). Thus

$$G(\lambda, x, y, z) = \frac{-1}{2\pi} \int_{-\infty}^{-2\lambda} \int_{-c}^{+c} \frac{F_{\xi} d\xi d\eta}{D'} - \frac{1}{2\pi} \int_0^{+\infty} \int_{-c}^{+c} \frac{F_{\xi} d\xi d\eta}{D'} \quad (7)$$

Then

$$\phi = U_\infty x + \phi_{\lambda=\infty} - U_\infty G(\lambda, x, y, z) \quad (8)$$

or in terms of the local velocities

$$\begin{aligned} u = \frac{\partial \phi}{\partial x} &= U_\infty + u_{\lambda=\infty} - U_\infty G_x(\lambda, x, y, z) \\ &= U_\infty(1 - G_x(\lambda, x, y, z)) + u_{\lambda=\infty} \end{aligned} \quad (9)$$

If an average value of G_x can be found, then

$$u = U_\infty(1 - \bar{G}_x) + u_{\lambda=\infty} \quad (10)$$

and the velocities (and therefore the forces) on a finite wing can be compared to the velocities and forces on an infinite wing. The forces will correspond if

$$U_\infty(1 - \bar{G}_x) \Big|_{\text{finite wing}} = U_\infty \Big|_{\text{infinite wing}} \quad (11)$$

Thus the quantity $U_\infty \bar{G}_x$ represents a difference or change in free-stream velocity between the finite and the infinite wing free-stream velocities. With signs chosen as shown,

$$\frac{\Delta U_\infty}{U_\infty} = U_\infty \Big|_{\text{finite wing}} - U_\infty \Big|_{\text{infinite wing}} / U_\infty = \bar{G}_x \quad (12)$$

Anderson in Reference 2 did carry out the averaging process over the finite wing planform to obtain $G_x(\lambda)$ for use in fixed-wing calculations. Because of the spanwise variation of flow over rotor blades, an average which is also a function of spanwise position (or distance from the tip) would be more useful for rotary wings. Therefore, the averaging will be carried out only over the chord. Since thin airfoil assumptions have been made, the evaluation may be done in the $r=0$ plane.

$$\bar{G}_x(\lambda, r) = (1/2c) \int_{-c}^{+c} G_x(\lambda, x, y, z=0) dx \quad (13)$$

Then the two-dimensional airfoil data now used in blade element analysis can be corrected at each element to give the equivalent three-dimensional data.

Derivation of the equations and the mathematical manipulations indicated are shown in detail in Reference 1. The indicated integration cannot be done analytically, and a Taylor series expansion of three terms is used. For helicopter rotor blades of the usual high aspect ratio, only the complementary wing near the tip need be considered. The result is

$$\bar{G}_x = \frac{\Delta U_\infty}{U_\infty} = \frac{1}{4\pi c} [h_1(c/y) I_1/c + h_2(c/y) I_2/c^3 + h_3(c/y) I_3/c^5] \quad (14)$$

where

$$h_1(c/y) = 2 \frac{\sqrt{(c/y)^2 + 1} - 1}{\sqrt{(c/y)^2 + 1}} \quad (15)$$

$$h_2(c/y) = \frac{1}{31} [4-2 \frac{6(c/y)^4 + 5(c/y)^2 + 2}{[(c/y)^2 + 1]^{5/2}}] \quad (16)$$

$$h_3(c/y) = \quad (17)$$

$$\frac{1}{51} [48-6 \frac{40[(c/y)^8 + (c/y)^6] + 63(c/y)^4 + 36(c/y)^2 + 8}{[(c/y)^2 + 1]^{9/2}}$$

The values of I_n/τ do not vary appreciably between differing airfoils, as they are geometric relations between the airfoil profile and the rectangle enclosing the profile. These values calculated for a parabolic arc airfoil are

$$\begin{aligned} I_1/\tau &= -1.333 \\ I_2/\tau &= -0.800 \\ I_3/\tau &= -0.571 \end{aligned} \quad (18)$$

This change in velocity has been derived for incompressible flows. The Prandtl-Glauert transformation is applied (in the manner described in pages 51 and 52 of Reference 1), resulting in the form

$$\Delta U_c/U_\infty = \frac{1}{4\pi Bc} \sum_n h_n(c/y) I_n/c^{2n-1} \quad (19)$$

The calculation of the value of $\Delta U_c/U_\infty$ has been programmed into a simple subroutine CORFAC described in the appendix. The number of terms of the Taylor series used can be varied. There is only a slight difference between using one or three terms, but since the computer time is only slightly increased, it is suggested that three terms be used. By adding the result found from replacing the variable c/y by $c/(2\lambda c - y)$, since $2\lambda c$ defines the span in feet, the effect of the opposite complementary wing is found, and a finite rather than a semi-infinite wing is represented. The use of a finite wing does not appear to have a significant effect; thus the use of the semi-infinite representation is suggested.

The velocity difference can be expressed in terms of a change in Mach number and in drag coefficient, by considering the compressible quasi-one-dimensional flow through a stream tube.

$$\Delta M/M_\infty = (1 + \frac{\gamma-1}{2} M^2) \Delta U/U_\infty = \Gamma \Delta U_c/U_\infty \quad (20)$$

$$\Delta C_D/C_D = - \frac{2-M^2}{1 + \frac{\gamma-1}{2} M^2} \Delta M/M \quad (21)$$

Thus, given the two-dimensional drag coefficient vs. Mach number plot, the three-dimensional characteristic can be found by using the above two equations as sketched in Figure 3 (a). We should note that the change in Mach number given by equation (20) causes a much larger change in drag coefficient in the subsonic drag rise range than the ΔC_D correction given in equation (21).

The technique as derived here gives the difference in flow characteristics between two- and three-dimensional, inviscid and nonlifting wings. Since it is the change that is calculated, the equations can be applied to viscous and lifting wings. The tip relief effect is primarily a displacement effect which is represented by the nonlifting wing.

THE USE OF THE TIP RELIEF CORRECTION IN STRIP ANALYSIS

Strip analysis calculations assume that each element can be considered aerodynamically as an independent two-dimensional airfoil segment at the velocities, Mach number, etc., present at the location of the element on the rotor disc. The tip relief correction changes the Mach number as per equation (20), and the drag coefficient is then found at this new effective Mach number. The drag coefficient is further corrected by the ΔC_D given by equation (21). No change is made for the lift or moment coefficients since the major difference between calculations and test is in terms of drag, although the technique can be applied to these other coefficients.

The application for the tip relief correction can best be described by the step-by-step outline given below. Instead of directly determining the drag coefficient as is now done in strip analysis, the following steps should be carried out:

1. Calculate the correction factor using equation (19) for the particular blade element.
2. Determine $M_{eff} = M_\infty + \Delta M$ using equation (20). (22)
3. Determine the drag coefficient $C_{D, eff, M}$ but at M_{eff} as is now done, all other parameters (α , R_e , etc.) remaining the same. This is the drag coefficient with Mach correction only, $C_{D, eff, M_{eff}}$.
4. Using equation (21), calculate the effective drag coefficient

$$C_{D, eff} = C_{D, eff, M_{eff}} (1 + \Delta C_D/C_D) \quad (23)$$

The signs used in equations (22) and (23) need some further explanation, as they may appear inconsistent. The reason is that the derivation of equations (15) through (21) is made to go from two-dimensional to three-dimensional characteristics, or vice versa. But the application described here is that given the three-dimensional flight parameters (i.e., Mach number) and the two-dimensional aerodynamic characteristic (namely, drag coefficient), determine the three-dimensional drag coefficient. This is shown in Figure 3 (b).

These steps have been incorporated into the strip analysis computer programs for rotor performance calculation that are used by the Eustis Directorate, USAAMRDL. These programs, one for hover and another for forward flight, use straightforward blade element strip analysis techniques (which will not be described here). These programs determine the airfoil characteristics by calling an external subroutine which stores the airfoil data. A simple option was added to the main programs either to call the airfoil subroutine as was done previously or to calculate the performance using tip relief by calling the subroutine TR whose listing is in the appendix. The subroutine TR calls the airfoil subroutine after determining the effective Mach number, but keeping all other parameters constant. The subroutine TR together with CORFAC carries out the steps listed above.

A number of runs have been made of these programs both with and without tip relief to determine the change in torque resulting from tip relief. The effect of the theory on the drag coefficient distribution is indicated in Figure 4. As expected, the drag is reduced more near the tip and as Mach number increases. The largest change by far is due to the change in Mach number rather than the change in drag coefficient from the tip relief theory. A further discussion of these results is postponed for a few pages so that comparison can be made with a simplified strip technique which may be used in energy type calculations.

A SIMPLIFIED BLADE ELEMENT ANALYSIS TO CALCULATE TIP RELIEF

By making a simplifying assumption concerning the variation of the drag coefficient with Mach number and another assumption on the two changes to the drag coefficient by the tip relief effect, a greatly simplified equation for the change in rotor torque due to tip relief is found. The result of these assumptions is a simplified integral for torque due to tip relief. The results can be used in a number of ways: as a general indication of the magnitude of the torque due to tip relief; empirically in performance calculations; or as part of an energy type computer program, since computing time for the integration routine is very short.

In a previous report¹, this approach was described for the hovering rotor. Here the approach is extended and results presented for a rotor in forward flight.

————— No Tip Relief
 - - - - - Tip Relief, Mach Correction Only
 - - - - - Tip Relief Correction

Rotor Data:
 2 Blades, Twist -8°
 $\sigma = 0.0468$
 $C_T/\sigma = 0.8$

(Note Scale Change)

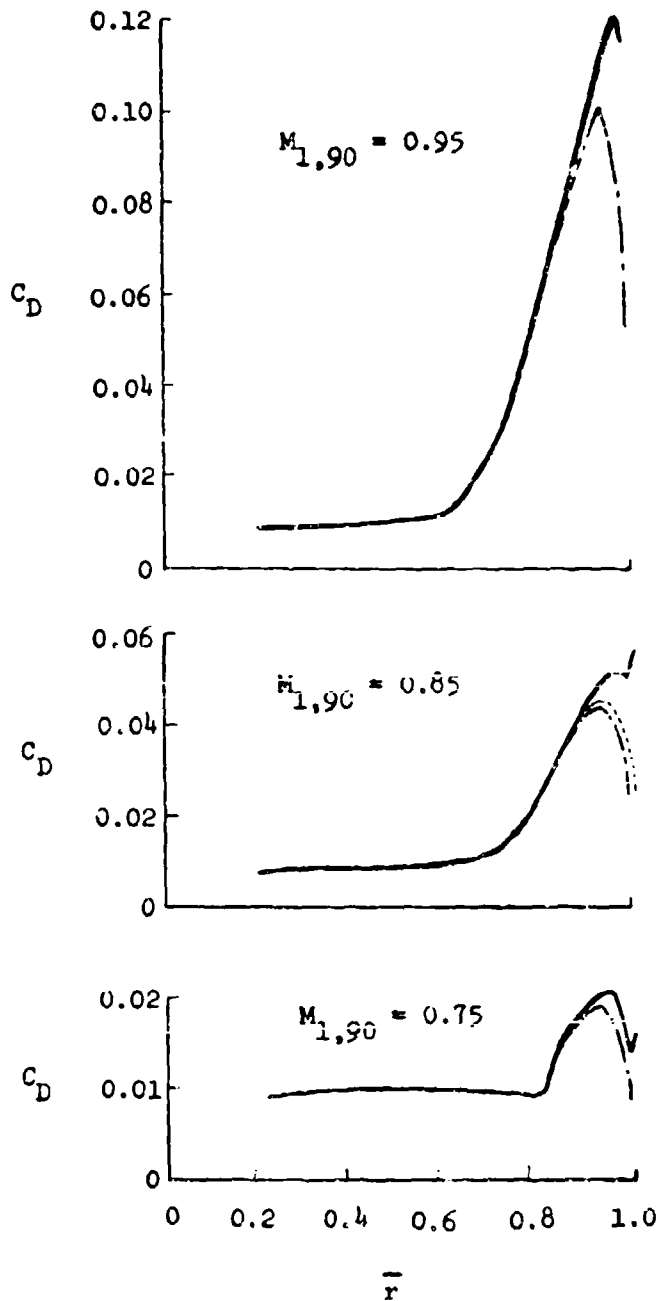


Figure 4. Drag Distribution on a Hovering Rotor.

The first assumption concerns the drag coefficient variation with Mach number. A very simplified representation, which has been often used, is by two straight lines as

$$C_D = C_{D_{inc}} \quad 0 < M < M' \quad (24)$$

$$C_D = C_{D_{inc}} + a_c (M - M') \quad M' < M < 1.0 \quad (25)$$

Here M' is an arbitrary Mach number to fit the approximation and $C_{D_{inc}}$ is the incompressible drag coefficient. Since $C_{D_{inc}}$ will drop out of the derivation, its value and variation around the rotor disc are immaterial. Typical values for an NACA 0012 airfoil section would be

$$\begin{aligned} M' &= 0.8 \\ a_c &= 0.57 \end{aligned} \quad (26)$$

The tip relief correction to the drag coefficient is made up of two parts: a change in the effective Mach number resulting in a change in the drag coefficient, and a change of the drag coefficient itself. The change in drag coefficient due to the change in effective Mach number has been found to be much larger than the change of the drag coefficient itself in the subsonic drag rise range. Therefore, the latter correction can be neglected. By neglecting this correction, there is no tip relief effect on the drag coefficient below M' , since the drag coefficient is independent of Mach number in this range. The equation for the drag coefficient for a finite wing, in the range M greater than M' , is the combination of the two-dimensional drag coefficient with the tip relief correction

$$C_{D_{FW}} = C_{D_{inc}} + a_c [(M - \Delta M) - M'] + \Delta C_D \quad (27)$$

The parameters ΔM and ΔC_D are the tip relief corrections. Neglecting the ΔC_D term and rearranging,

$$\begin{aligned} C_{D_{FW}} &= C_{D_{inc}} + a_c [M - M' - \Delta M] \\ &= C_{D_{inc}} + C_{D_c} + C_{D_{TR}} \end{aligned} \quad (28)$$

where

$$\begin{aligned} C_{D_{inc}} &= \text{Incompressible two-dimensional drag coefficient} \\ &\quad \text{of the section} \\ C_{D_c} &= \text{Drag due to compressibility effects in two-dimensional} \\ &\quad \text{flow} = a_c (M - M') \end{aligned}$$

$$C_{D_{TR}} = \text{Drag due to the tip relief effect} = a_c \Delta M$$

Using equations (19) and (20) and $C_{D_{TR}}$ as defined above for equation (28),

$$C_{D_{TR}} = a_c \Delta M = a \Gamma (1/\beta) (\tau/4\pi) [\Sigma h_D (\beta c/y) L_D / \tau] M \quad (29)$$

Since the drag coefficient variation with Mach number is taken to be linear and is broken into its components, one being the tip relief drag coefficient, the torque coefficient on a rotor blade may be similarly broken into its components. The component we are concerned with is torque due to tip relief. With the usual assumptions concerning small angles, no radial flow, etc., the torque of an element of a rotor blade due to drag is

$$\begin{aligned} dQ &= r dD \\ &= \frac{1}{2} \rho (\Omega r + V \sin \psi)^2 C_D 2c r dr \end{aligned} \quad (30)$$

Since the equation for the drag coefficient is linear, the change in torque due to tip relief on the element may be written as

$$dQ_{TR} = \frac{1}{2} \rho (\Omega r + V \sin \psi)^2 C_{D_{TR}} 2c r dr \quad (31)$$

Transforming to coefficient form,

$$dC_{Q_{TR}} = \frac{1}{2} \rho \frac{(\Omega r + V \sin \psi)^2}{\pi R^2 \rho (\Omega R)^2 R} C_{D_{TR}} 2c r dr \quad (32)$$

with Prandtl-Glauert transformation for solidity

$$\sigma_c = b 2c_c / \pi R = 2b / \pi R c_1 \beta = \beta \sigma_1 \quad (33)$$

and the definition of advance ratio, μ

$$dC_{Q_{TR}} = (1/2) (\sigma_1 / b \beta) (\mu \sin \psi + \bar{r})^2 C_{D_{TR}} \bar{r} d\bar{r} \quad (34)$$

The change in torque per blade due to tip relief is found by integrating the elemental torque along the blade span and averaging around the azimuth. Mathematically this is expressed as

$$Q = \frac{1}{2\pi} \int_0^{2\pi} \int_0^R \frac{dQ}{dr} dr d\psi \quad (35)$$

Thus

$$\frac{C_{Q_{TR}} / b}{\sigma / b} = \frac{1}{4\pi} \int_0^{2\pi} \int_0^1 \frac{1}{\beta} (\mu \sin \psi + \bar{r})^2 C_{D_{TR}} \bar{r} d\bar{r} d\psi \quad (36)$$

Now C_{DTR} is given by equation (29) for the case where only the ΔM effect of tip relief is used.

$$\frac{C_{DTR}}{\sigma/b} = \frac{1}{4\pi} \int_0^{2\pi} \int_0^1 (\nu \sin \psi + \bar{r})^2 a_c \frac{\Gamma}{\beta^2} \frac{\tau}{\bar{r}} \quad (37)$$

$$\left[\Sigma h_n \left\{ \frac{\beta c}{y} \right\} \frac{I_n}{\tau} \right] M \bar{r} d\bar{r} d\psi$$

If this equation is restricted to hover and to only the first term of the Taylor series, it will reduce to equation (122) of Reference 1, which is

$$C_{DTR} = \frac{\sigma a_c}{4\pi} \left(\frac{I_1}{\tau} \right) \int_0^1 \frac{M \bar{r}^3}{\beta^2} \left(1 + \frac{\gamma-1}{2} M^2 \right) \left[1 - \frac{1}{\sqrt{\left(\frac{1}{(2\beta y \lambda_c (1-\bar{r}))^2} + 1 \right)^2 + 1}} \right] d\bar{r} \quad (37a)$$

The integration and calculation of this equation are done by the use of the computer programs TRDRIVER, TIPRLF and CORFAC. (See appendix.) The programs are set up so that the latter two subprograms may be used with an energy type program, while TRDRIVER will drive the two subprograms so that the tip relief effect can be evaluated by itself. The program TIPRLF carries out the integration using a rectangular formula as

$$\int_0^1 \int_0^{2\pi} f(\bar{r}_1, \psi) d\bar{r} d\psi = \sum_i \sum_j f_{i,j}(\bar{r}_1, \psi_j) \Delta \bar{r}_1 \Delta \psi \quad (38)$$

where

$$\Delta \psi = 2\pi/n_\psi \quad \psi_j = j\Delta\psi, \quad j = 0, 1, \dots, n_\psi \quad (39)$$

$$\Delta \bar{r}_1 = \bar{r}_1 - \bar{r}_{1-1} \quad \bar{r}_1^1 = (\bar{r}_1 + \bar{r}_{1-1})/2$$

and the values of \bar{r}_1 and n_ψ are input to the program. The tip relief driver has three sets of \bar{r}_1 listed. The program was debugged using the first set of 10 \bar{r}_1 's. Comparison with the second set of \bar{r}_1 's, with 30 values, indicated a big difference, but comparison of the third set of 15 values and the second set showed only a slight difference. Similarly, a comparison of 24 and 36 azimuthal stations did not show any significant differences.

The cost of computation using these subroutines is minimal. In calculating the plots presented here on a DEC PDP-10 computer, some seventy-five flight conditions could be calculated in less than two minutes of CPU time at a cost of approximately three dollars including compilation.

TIP RELIEF EFFECT ON PERFORMANCE

In the previous sections of this chapter, we have described a theory for the quantitative determination of the tip relief and two calculative techniques. In this section, results from these calculations are shown. The results from the simplified theory are presented first, as these results cover a wider range of parameters. The number of calculations using the various strip methods was limited due to time and cost; the results from the strip analyses are given and compared to the simplified theory.

We should note that the equation derived (see equation (37)) has as the result

$$\frac{C_{Q_{TR}}}{(\sigma/b)} \text{ per blade}$$

which is identical in magnitude to the quantity

$$\frac{C_{Q_{TR}}}{\sigma}$$

but the first quantity indicates that the major parameter of tip relief is solidity per blade (σ/b). This is related to blade aspect ratio by

$$\lambda = \frac{b}{\pi r} \quad (40)$$

where the blade aspect ratio, λ , is defined as the rotor radius to chord ratio. Only rectangular planforms are considered herein. Figures 5 and 6 show the variation of the tip relief torque with advancing tip Mach number, rotational Mach number, and advance ratio as calculated by the simplified method. The two figures differ in blade aspect ratio.

These figures show a map of the tip relief torque variation with flight variables. Lines of constant rotational Mach number ($\Omega R/a$) would be obtained as a helicopter gained forward speed at a constant rotational speed (Ω) and at constant temperature. As the forward speed is increased from hover, in general the torque due to tip relief increases slowly. In some cases of low (only slightly above M') rotational and advancing tip Mach numbers there may even be a decrease. The slow rise or decrease in torque occurs because as the Mach number decreases on the retreating side, the tip relief effect is also reduced, while there is the increase in Mach number and tip relief torque on the advancing side. Their balance determines the magnitude of the decrease and the rate of rise of tip relief torque at these low forward speeds. After the Mach number on the retreating side has decreased to a negligible value, the Prandtl-Glauert type effect becomes dominant and $C_{Q_{TR}}$ rises.

At very moderate advance ratios, above about 0.10 to 0.15, the curves coalesce and become independent of either rotational Mach number or advance ratio. A line indicating the lower envelope of these points has been drawn, which is used in the following comparisons, and is labeled "high-speed envelope".

Thus, as far as tip relief is concerned, at rotational tip Mach numbers below M' , the value of the tip relief torque depends mainly on advancing tip Mach number and only slightly (for practical purposes, negligibly) on advance ratio or $\Omega R/a$.

Figure 7 indicates how tip relief varies with various parameters and compares calculative techniques and some limited test data. This is discussed in detail in the following paragraphs.

The extremes of these two sets of curves from Figures 5 and 6, the hover and the high-speed envelope, are replotted in Figure 7(a) to show the effect of solidity per blade on the tip relief torque. The tip relief is calculated for a semi-infinite wing tip relief model, it does depend, to an important degree, on aspect ratio.

The key parameter for tip relief is distance from the tip in terms of chord and local Mach number. The tip relief effect diminishes rapidly with distance from tip. The rotor blade with the greater chord (i.e., lower aspect ratio, a higher solidity per blade), will have an element at the same r , and thus the same Mach number, closer to the tip in terms of chord than a blade with a shorter chord. This element will therefore have a larger tip relief correction. Thus the blade with the greater chord will have greatest tip relief and the larger alleviation of compressible power loss, other things being equal.

Figures 7(a), (b) and (c) present comparisons between the simplified calculation, strip analysis and some flight test data. These comparisons must be analyzed with care, as all of the methods have certain problems associated with them. The simplified calculations take too few points near tip Mach numbers of 0.80 and diverge greatly near Mach one due to the Prandtl-Glauert effect. The two-dimensional airfoil data at high subsonic Mach numbers may not be as valid as one would like.

In hover (Figure 7(b)), the simplified theory gives a much higher value of tip relief than does strip analysis. On the other hand, at a high advance ratio, the agreement, as shown in Figure 7(c), could not be better. No explanation for this discrepancy and this agreement has been found. But note that computation for both cases was made only in the range of 0.82 to 0.89 in advancing tip Mach numbers.

Presented in Figure 7(d) is some comparison with test data. The method of determining the experimental values of torque due to tip relief requires some detailed explanation. Reference 3⁴ (specifically in Figure 9) presents both test data and theoretical calculations for the

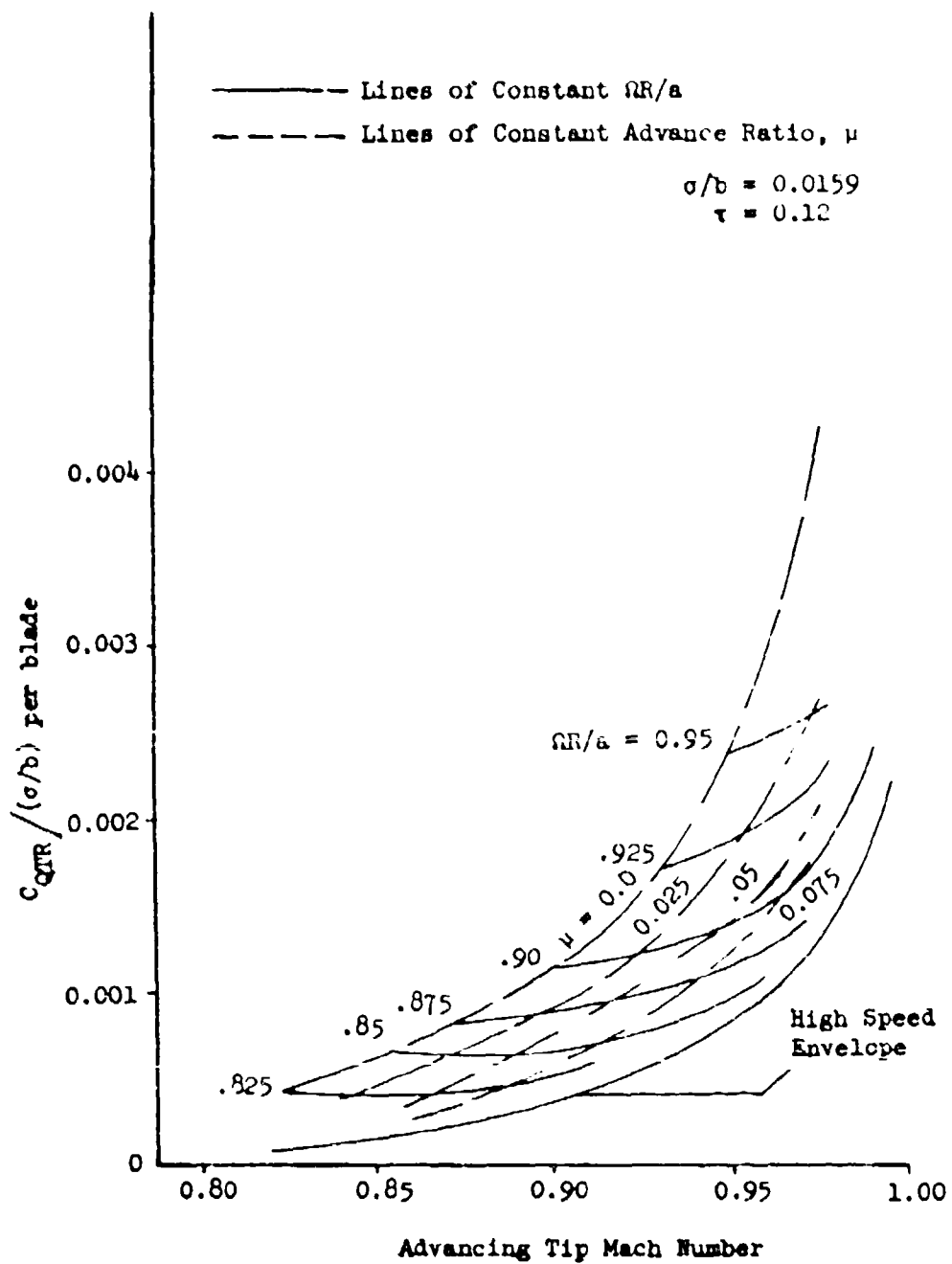


Figure 5. Change in Torque Coefficient Due to Tip Relief ($\sigma/b = 0.0159$).

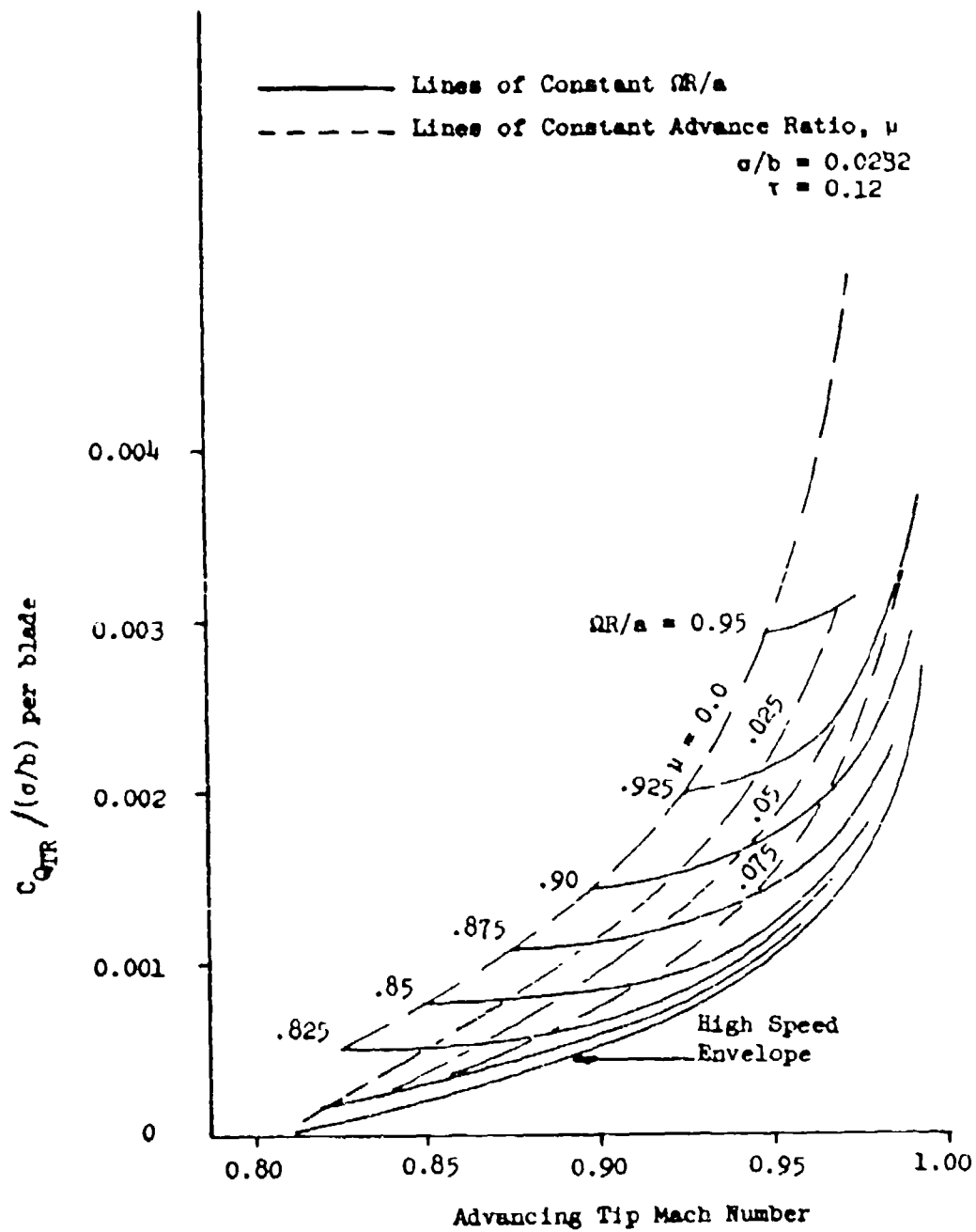
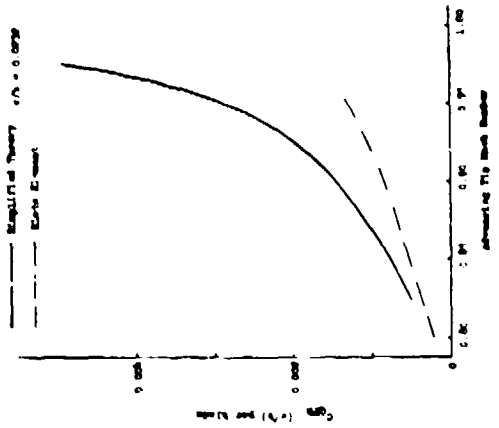
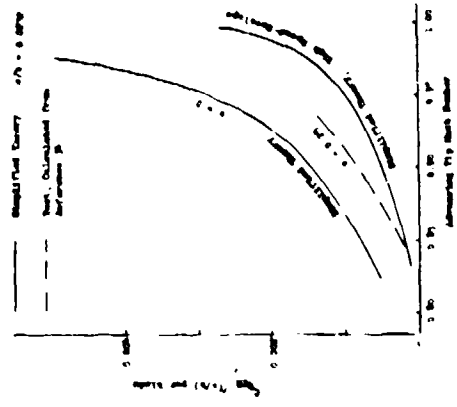


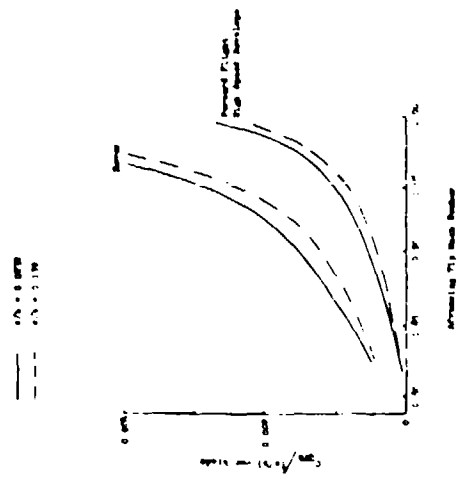
Figure 6. Change in Torque Coefficient Due to Tip Relief ($\sigma/b = 0.0232$).



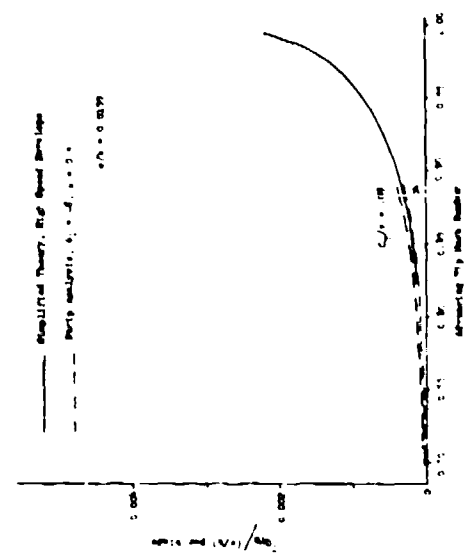
(a) Effect of Solidity, Simplified Theory.



(b) Comparison of Calculative Techniques in Hover.



(c) Comparison of Calculative Techniques in Forward Flight.



(d) Comparison of Simplified Theory to Flight Test Data.

Figure 7. Change in Torque Coefficient Due to Tip Relief, Some Comparisons.

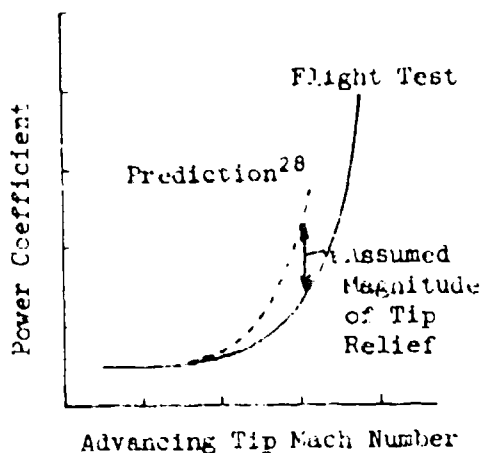


Figure 8. Typical Comparison of Test and Predicted Power Required.³⁴

variation of the power coefficient with advancing tip Mach number for the UH-1F helicopter at $\mu = 0.25$. The test data is presented as a curve (as opposed to data points) and includes instrument corrections, cross plotting, fairing, etc. Performance prediction is based on Tanner²⁸ and includes the solidity correction. The full difference between the power required test data of Reference 9 and the calculated value from the Tanner charts²⁶ is attributed to the tip relief effect. A typical curve³⁴ and the power attributed to tip relief are sketched in Figure 8. Since in magnitude $C_p = C_Q$, the value of C_{QTR} determined in this manner is divided by σ and replotted in Figure 7(d), it is surprising that

the test data increases with advancing tip Mach number more rapidly than the theory would predict.

It should be noted in regard to the accuracy required that the calculation is of the change in torque coefficient due to tip relief. The order of magnitude of C_Q is about 25×10^{-5} , while at the same time the change in torque coefficient due to tip relief is about 2×10^{-5} . Thus, there is a factor of 10 between these two numbers, which are subtracted from each other. Three-place accuracy on ΔC_{QTR} requires four-place accuracy of C_Q .

The results of the theory overall appear to be useful in performance calculations. Some more detailed calculations are needed to resolve some anomalies, especially calculations using strip theories. Also, further comparisons with test data would be useful.

TIP RELIEF COMBINED WITH COMPRESSIBILITY

It should be emphasized that the calculation of the tip relief as presented here is not a calculation of the effect of compressibility; rather, it is a correction to the calculation of compressibility effects, as presently used for rotor performance calculations using two-dimensional airfoil data. In strip analysis, tip relief corrects the two-dimensional compressible flow airfoil coefficients. In energy type calculations, care must be taken to be sure that tip relief is not already included in the method used to calculate compressibility power losses. For example, empirical curves fitted to test data will by definition include the tip relief effect.

To indicate the importance of this point, the calculation of power loss due to compressibility from Reference 32 has been combined with the

simplified tip relief calculation as presented here. Gessow and Crim³² calculated the compressible power loss using a strip analysis²⁷ with compressible airfoil data. The compressible power loss is defined as the difference between the power at a low and a high tip speed. Figure 9 indicates the results of Gessow and Crim,³² later calculations presented by Dingeldein,⁴⁵ flight test results,³³ and the combined compressibility and tip relief power loss.

The key result of calculating the compressibility power loss of Gessow and Crim³² for a series of advance ratios (from 0.2 to 0.5), twists (0° , -8° and -16°), and solidities (0.025 to 0.08) was that the most important parameter is the difference between the advancing tip Mach number and the drag divergence Mach number ($M_{1,90} - M_{dd}$). They drew a single, best-fit curve through the calculated point on a C_{pc}/σ vs. $M_{1,90} - M_{dd}$ plot. This is the curve labeled in Figure 9 as being from Reference 32. We should note that the scatter is of the order of ± 0.001 in C_{pc}/σ , which is one division on the ordinate scale. Reference 45 found an even larger spread, as indicated by the two limit curves in Figure 9.

The high-speed envelope value of C_{QTR}/σ is subtracted from that of Gessow and Crim³² to obtain the tip relief corrected compressibility tip power loss curves. Mean values of C_{QTR}/σ from the two solidities (0.0159 and 0.0232 of Figures 5 and 6) are used, as the other curves represent a wide range of solidities. For the first curve we used $M' = M_{dd} = 0.80$ (Curve 1). But M_{dd} in Reference 32 at zero angle of attack is about 0.74; therefore, C_{QTR}/σ was also calculated with $M' = 0.74$ and using $a_c = 0.492$ to represent the airfoil (Curve 2).

The tip relief corrected compressibility power loss becomes almost a straight line in both cases when plotted against $M_{1,90} - M_{dd}$ (Figure 9). The Prandtl-Glauert law increases the tip relief at the same rate that compressibility increases the power loss. When compared to the AFFTC flight test results,³³ the prediction is still greater than the test values which would be expected to include tip relief. For a more complete comparison, a better representation of the drag coefficient than equation (25) is needed.

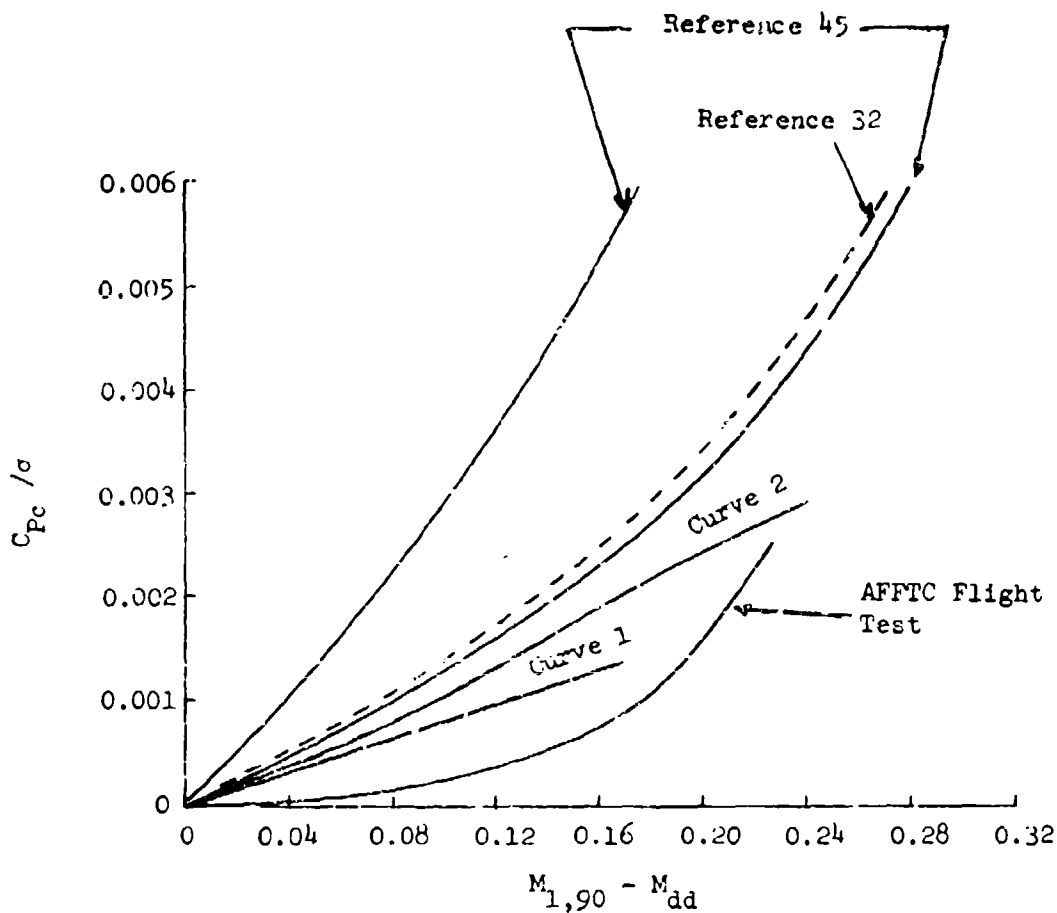


Figure 9. Comparison of Compressibility Effects.

TIP RELIEF CALCULATION AS PROPOSED BY PROUTY

Theory - Description, Discussion and Critique

In the October 1971 issue of the AHS Journal, Prouty⁴⁶ described a simple, empirical means of calculating the magnitude of the tip relief effect. The approach states that the apparent three-dimensional drag divergence Mach number on a rotor differs from the two-dimensional measured drag divergence Mach number of a "correction" which was previously developed by Sopher.⁵ A further empirical multiplication factor for the forward-flight case accounts for the fact that "until a significant portion of the blade dwells in a region of drag divergence

for a significant time the effects are not apparent in measurements of power."

This is similar to the simplified method presented here, in that a correction to the Mach number is made. The nature of the blade element integration will account for the second factor.

An examination of Prouty's approach to tip relief appears to indicate that it is based on a theory which is not applicable to the problem. In the following paragraphs, the Mach number correction as proposed by Prouty will be described along with its theoretical basis and the reasons for doubting its theoretical validity.

Prouty applies the correction to the drag divergence Mach number, but he indicates that the correction can be applied to other than this particular value of the Mach number. The Prouty correction factor is

$$\sqrt{1 - \bar{C}_{P_{inc}}}$$
 (41)

where $\bar{C}_{P_{inc}}$ is an average incompressible-flow airfoil pressure coefficient. For the basis of using this correction factor, Prouty simply states that it was derived in Sopher's work,⁵ who in turn refers to Kùchemann and Weber.⁴⁷

A relationship between the theoretical potential flow equations for compressible flow and those for incompressible flow is the Prandtl-Glauert transformation

$$\beta^2 = 1 - M_\infty^2$$
 (42)

A further refinement for a transformation between theoretical compressible flow and theoretical incompressible flow was developed by Kùchemann and Weber⁴⁷ and is given as

$$\beta^2 = 1 - M_\infty^2 (1 - \bar{C}_{P_{inc}})$$
 (43)

In the original paper,⁴⁷ it was suggested that $\bar{C}_{P_{inc}}$ should be a suitable chosen mean value of the pressure coefficient over the suction region of the airfoil in incompressible flow. Later similar extensions of the Prandtl-Glauert transformation all use the incompressible pressure coefficient but suggest that the local rather than a mean value be used (for example, Lock, et al⁴⁸).

The extension of the Kùchemann-Weber rule to rotors was made by Sopher⁵ by use of a so-called "equivalent linear theory tip Mach number." If $\bar{C}_{P_{inc}}$ is a constant, then the quantity $M_\infty \sqrt{1 - \bar{C}_{P_{inc}}}$ can be considered as a "equivalent" Mach number. In the case of a rotor, M_∞ is replaced by $\Omega R/a$, and thus $(\Omega R/a) \sqrt{1 - \bar{C}_{P_{inc}}}$ would represent an "equivalent linear theory tip Mach number."

Equation (43) was derived for compressible, two- and three-dimensional flow over airfoils and wings, and is the transformation between theoretical compressible flows and an equivalent incompressible flow. It is not related in any way that we can determine to any relation between two- and three-dimensional flows.

In conclusion, the applicability of the theoretical basis for Prouty's approach to tip relief is doubtful.

DISCUSSION OF SIMILARITY LAWS FOR ROTORS

The concept of similarity laws is important for the application of fluid mechanics in design practice. The governing differential equation of fluid motion lends itself to a solution only in rare, simplified instances. But an examination of these equations and the boundary conditions can lead to similarity laws which can then be used to assess the effects of varying various characteristics of the flow.

Similarity laws group the parameters (including nondimensional parameters) of the flow into functional groups, while dimensional analysis gives only the nondimensional parameters such as thickness ratio, Mach number, etc. The best known of the similarity laws is the Prandtl-Glauert law. Because the Prandtl-Glauert law is derived only on the basis of a linearized, homogeneous equation, it may be stated in a number of ways, for example,

$$C_P = C_{P_{inc}} \left(\frac{\tau}{\sqrt{1-M^2}} \right) \quad (44)$$

for a two-dimensional airfoil section. In this form, the Prandtl-Glauert law states that the pressure distribution will be the same for a family of airfoils of different thicknesses at different Mach numbers if the quantity $\tau/\sqrt{1-M^2}$ is kept constant. The pressure distribution, of course, when properly integrated, gives the drag, lift and moment; therefore, the functional variable for drag, lift and moment is very similar to the form given in equation (44).

The speed range of interest for high-speed helicopter rotors is the high subsonic and transonic region. Similarity laws for transonic flows were developed by a number of investigators; a complete description and bibliography is given by Spreiter.⁴⁹ The transonic similarity rule for drag is

$$\tilde{C}_D = \tilde{C}_D(\tilde{M}, \tilde{\lambda}) \quad (45)$$

where

$$\begin{aligned} \tilde{C}_D &= \frac{[M^2(\gamma+1)\tau]^{1/3}}{\tau^{5/3}} C_D \\ \tilde{M} &= \frac{(M^2-1)}{[M^2(\gamma+1)\tau]^{2/3}} \\ \tilde{\lambda} &= [M^2(\gamma+1)\tau]^{1/3} \lambda \end{aligned}$$

The quantities given by \tilde{C}_D , \tilde{M} and $\tilde{\lambda}$ are called reduced drag coefficient, reduced Mach number, and reduced aspect ratio. Because of the functional nature of the similarity rule, this relation may be given in somewhat different forms. The similarity rule simply states that a plot of \tilde{C}_D against either \tilde{M} or $\tilde{\lambda}$, while holding the other constant, will result in a single curve. The similarity rule by itself does not give the

equation for this curve. It may be possible to empirically cross-plot airfoil data and, for certain ranges, obtain an equation relating the reduced variables.

The tip relief theory for either fixed wings² or rotary wings¹ is a similarity law, in that they give the relationship of the drag variation between two- and three-dimensional airfoils. The theory as derived is not in a functional form, but in application the tip relief theory does reduce the number of curves required to present the information. For example, to present the drag coefficient of wings of different aspect ratios, a separate curve would be required for each aspect ratio. By applying the correction factor from the theory, this same set of data can be presented as a single curve.² This differs from the usual application of similarity rules where the data is presented with a new set of coordinates.

The possibility of comparing the results of the similarity rule given by the tip relief theory and the conventional transonic similarity rule has been investigated without any success to date. A notable feature of the transonic similarity rule relating drag coefficient to aspect ratio is that thickness is raised to powers other than the first in the functional variable, as is shown in the example for drag in equation (45). On the other hand, the tip relief theory, based as it is on linearized airfoil theory and the linearized, elliptic equation of subsonic flow transformed to the equivalent incompressible equations, gives a variation of thickness ratio to the first power.

Further work in applying transonic similarity laws to helicopter rotor aerodynamics is needed. Derivation of similarity rules for rotors, such as those available for fixed wings, would be very useful, but it appears to be more in the way of a long-term goal. More immediate applications would include tests of the validity of the airfoil data now in use and their extension to higher speeds, and the use of similarity rules to describe airfoil data in energy type calculations. This latter application would extend the present use of two-dimensional data in rotor aerodynamics by use of the transonic similarity rules.

COMMENTS ON EXPERIMENTAL VERIFICATION OF
COMPRESSIBILITY EFFECTS AND TIP RELIEF

There is solid theoretical evidence of the existence of a compressibility tip relief effect on helicopter rotors. There are similar experimental trends to that effect. Assuming the theoretical model to be sound, it would be desirable to design the definitive experiment to "calibrate" tip relief. This presents great difficulties, which will be discussed here.

Tests for the overall tip relief effect for fixed wings in uniform flow were described in Reference 50, where very good correlation was found. In the extension¹ to rotary wings, two steps are used: First the variation of the tip relief correction along the span is calculated for uniform flow. The second step combines this variation with blade element theory; namely, the tip relief correction of a particular element in a rotor is the same as the tip relief of the element in a fixed wing that is located at the same distance from the tip in a flow having the free-stream velocity of the blade element. The Mach number, Reynolds number, angle of attack, etc., are also the same for the two elements. Thus there are two hypotheses that need experimental verification.

Tests of the spanwise variation of the tip relief effect could be performed in a very large transonic wind tunnel. Since the effect is mainly in the first chord length near the tip, one would need the detailed drag distribution in this region. The need for a large chord so as to be compatible with the instrumentation, followed by the need for a reasonable aspect ratio and a large throat to avoid interference, would require an enormous wind tunnel. As a beginning in testing for the tip relief effect, local pressure distributions would be useful. Systematic measurements of the pressure distribution on wings of various aspect ratios at high Mach numbers are needed. At incompressible speeds, some data of this nature is available,⁵¹ but the change due to tip relief is less than the accuracy of the experiment, and comparison is not possible. Compressible airfoil data appear to be mostly measured by balances.^{52,53}

Tests of the application to rotors, by systematic variation of parameters which effect the tip relief without changing other aspects of rotor performance, would be more intellectually satisfying.

As stated several times in this report, tip relief is correction to the present calculation of compressibility effects. Assuming that one can differentiate in a given set of test data between incompressible and compressible power, one must further be able to fully account for changes in two-dimensional compressibility effects before one can calculate the three-dimensional effects, i.e., tip relief. Today, for example, reliable two-dimensional test results for the 0012 airfoil at Mach numbers up to one are not yet available. It can be said that

detailed information on helicopter rotor compressibility effects is sketchy at best. The determination of tip relief therefore requires trustworthy calculation of the rotor performance based on blade element analysis.

Since the tip relief compressibility effects are localized near the tip, it is tempting to try to test a blade tip element in a stationary position, with a spanwise-varying simulated flow, at transonic speeds. We were not able to come up with a reasonable wind-tunnel configuration to accomplish this objective, and we conclude that any tip relief tests must be made with a rotating blade and a constant free-stream flow, or in hover.

In this report, limited comparison to flight test data is made (Figure 7(d)). There is an increasing amount of flight test data at compressible tip speeds becoming available, and similar comparisons of these data are recommended. Time did not allow these comparisons to be performed, because no time was allotted to calculate the performance of the available flight test cases using present performance prediction methods. The experimental value of tip relief is taken as the difference between the calculated prediction and the measured power required. This leaves possibilities for errors in a number of ways, including the estimate of fuselage drag, and the effects of variable induced velocity, blade flexibility and unsteady effects. Thus in the flight test data, differences due to other causes may be thought of as errors in the tip relief theory.

In principle, one can verify tip relief in a manner similar to that used by Anderson^{2,50} in the fixed-wing case. This requires the use of three or more physically different rotors. Each rotor is identified by its blade aspect ratio, or σ/b . Preferably, σ/b should vary as much as possible for the three rotors, say, at least by a factor of 2 to 1. One then measures (and calculates from strip analysis) C_Q/σ against $M_{1,90}$ for various Mach numbers, say, between 0.7 and 0.9, at a constant C_T/σ . Assuming now that one has three rotors, identical except for the parameter σ/b , each has a different C_Q/σ against $M_{1,90}$ curve, for a given C_T . However, these curves should superimpose if the tip relief correction of this report is applied. This method can be used either for wind-tunnel tests or for flight tests.

CONCLUSIONS AND RECOMMENDATIONS

The methods used to calculate the effects of compressible flow on the performance of helicopter rotors have been reviewed. The application of a theory for tip relief based on the complementary wing concept has been described, and results from various applications have been given.

The results of the calculation and tip relief by the complementary wing theory indicate that the technique can and should be included in blade element type rotor programs. This is done by modifying the two-dimensional airfoil data now being used by the technique presented here to obtain three-dimensional airfoil data, which better represents the actual three-dimensional flow. Simplification of the strip analysis and the tip relief theory allows the calculation of the power associated with tip relief using a very quick computer program. These results match reasonably well with both tests and the more complex strip programs; thus this simplified technique should also be included in energy type calculations when combined with proper representation of the compressibility power required.

More work is needed in this area of properly predicting the performance of rotors operating in the compressible flow regime. There is available a large body of test data, including the work of Carpenter at NACA-Langley, the Edwards flight tests, and the NASA Ames wind tunnel tests, and a systematic comparison of the various prediction techniques reviewed here with this range of test data is needed. By making such a systematic comparison, the best of the prediction techniques can be chosen and developed for use in strip and energy calculations.

LITERATURE CITED

1. LeNard, John M., A THEORETICAL ANALYSIS OF THE TIP RELIEF EFFECT ON HELICOPTER ROTOR PERFORMANCE, Aerophysics Company; USAAMRDL Technical Report 72-7, Eustis Directorate, U.S. Army Air Mobility Research and Development Laboratory, Fort Eustis, Virginia, August 1972, AD 750 179.
2. Anderson, Gordon F., ASPECT RATIO INFLUENCE AT HIGH SUBSONIC SPEEDS, Journal of Aeronautical Sciences, Vol. 23, No. 9, September 1956, pp. 874-878. Also Brown University Technical Note WT-13; Air Research and Development Company, Office of Scientific Research OSR TN-55-232, July 1955, AD 49 365.
3. Simonov, L. A., and Kristianovich, S. A., INFLUENCE OF AIR COMPRESSIBILITY ON INDUCTIVE VELOCITIES OF AN AIRFOIL AND AIRSCREW, Prickladnoi Matematika i Mekhanika (USSR), Vol. VIII, No. 2, February 1944, pp. 89-88.
4. Burns, J. C., AIRSCREWS AT SUPERSONIC FORWARD SPEEDS, The Aeronautical Quarterly, Vol. III, No. 5, May 1951, pp. 23-50.
5. Sopher, Robert, THREE-DIMENSIONAL POTENTIAL FLOW PAST THE SURFACE OF A ROTOR BLADE, United Aircraft Corporation, Sikorsky Aircraft Division; Proceedings of the 25th Annual National Forum of the American Helicopter Society, Paper No. 324, May 1969.
6. Caradonna, Frank X., and Isom, Morris P., SUBSONIC AND TRANSONIC POTENTIAL FLOW OVER HELICOPTER ROTOR BLADES, AIAA Paper No. 72-39, Presented at the 10th Aerospace Sciences Meeting, San Diego, California, January 17-19, 1972.
7. Sears, W. R., POTENTIAL FLOW AROUND A ROTATING CYLINDRICAL BLADE, Journal of the Aeronautical Sciences, Vol. 17, No. 3, March 1950, pp. 184-185.
8. Hicks, J. C., and Nash, J. F., THE CALCULATION OF THREE-DIMENSIONAL TURBULENT BOUNDARY LAYERS ON HELICOPTER ROTORS, Lockheed-Georgia Research Laboratory, NASA CR-1845, May 1971.
9. Clark, David R., and Arnoldi, Douglas R., ROTOR BLADE BOUNDARY LAYER CALCULATION PROGRAMS, United Aircraft Corporation, Sikorsky Aircraft Division; USAAVLABS Technical Report 71-1, Eustis Directorate, U.S. Army Air Mobility Research and Development Laboratory, Fort Eustis, Virginia, March 1971, AD 723 989.
10. Goorjian, Peter M., and McCroskey, W. J., POTENTIAL FLOW AROUND A ROTATING BLADE, American Institute of Aeronautics and Astronautics Journal, Vol. 8, No. 12, December 1970, pp. 2303-4.

11. Landgrebe, Anton J., AN ANALYTICAL METHOD FOR PREDICTING ROTOR WAKE GEOMETRY, Journal of the American Helicopter Society, Vol. 14, No. 4, October 1969, pp. 20-32.
12. Landgrebe, Anton J., and Cheney, Marvin C., Jr., ROTOR WAKES - KEY TO PERFORMANCE PREDICTION, in AGARD Conference Proceedings No. 111, Aerodynamics of Rotary Wings, September 1972.
13. Gutsche, F., VERSUCHE AN UMLAUFENDEN FLUGELSCHNITTEN MIT ABGERISSENER STRÖMUNG, Jahrbuch der Schiffbautechnischen Gesellschaft, Vol. 41, Chapter VII, 1940.
14. Gustafson, F. B., THE APPLICATION OF AIRFOIL STUDIES TO HELICOPTER ROTOR DESIGN, NACA TN 1812, 1949.
15. Carpenter, Paul J., EFFECTS OF COMPRESSIBILITY ON THE PERFORMANCE OF TWO FULL-SCALE HELICOPTER ROTORS, NACA Report 1078, 1952 (Supersedes NACA TN 2277, 1951).
16. Shivers, J. P., and Carpenter, Paul J., EXPERIMENTAL INVESTIGATION ON THE LANGLEY HELICOPTER TEST TOWER OF COMPRESSIBILITY EFFECTS ON A ROTOR HAVING NACA 63₂-015 AIRFOIL SECTIONS, NACA TN 3850, December 1956.
17. Powell, Robert D., Jr., COMPRESSIBILITY EFFECTS ON A HOVERING HELICOPTER ROTOR HAVING AN NACA 0018 ROOT AIRFOIL TAPERING TO AN NACA 0012 TIP AIRFOIL, NACA RM L57F26, September 1957.
18. Jewel, Joseph, W., Jr., and Harrington, Robert D., EFFECT OF COMPRESSIBILITY ON THE HOVERING PERFORMANCE OF TWO 10-FOOT-DIAMETER HELICOPTER ROTORS TESTED IN THE LANGLEY FULL-SCALE TUNNEL, NACA RM L58B19, April 1958.
19. Powell, Robert D., Jr., and Carpenter, Paul J., LOW TIP MACH NUMBER STALL CHARACTERISTICS AND HIGH TIP MACH NUMBER COMPRESSIBILITY EFFECTS ON A HELICOPTER ROTOR HAVING AN NACA 0009 TIP AIRFOIL SECTION, NACA TN 4355, July 1958.
20. Shivers, James P., and Carpenter, Paul J., EFFECTS OF COMPRESSIBILITY ON ROTOR HOVERING PERFORMANCE AND SYNTHESIZED BLADE-SECTION CHARACTERISTICS DERIVED FROM MEASURED ROTOR PERFORMANCE OF BLADES HAVING NACA 0015 AIRFOIL TIP SECTIONS, NACA TN 4356, September 1958.
21. Carpenter, Paul J., LIFT AND PROFILE-DRAG CHARACTERISTICS OF AN NACA 0012 AIRFOIL SECTION AS DERIVED FROM MEASURED HELICOPTER-ROTOR HOVERING PERFORMANCE, NACA TN 4357, September 1958.
22. Powell, Robert D., Jr., MAXIMUM MEAN LIFT COEFFICIENT CHARACTERISTICS AT LOW TIP MACH NUMBERS OF A HOVERING HELICOPTER ROTOR HAVING AN NACA 64₁A012 AIRFOIL SECTION, NASA MEMO 1-23-59L, February 1959.

23. Jewel, Joseph W., Jr., COMPRESSIBILITY EFFECTS ON THE HOVERING PERFORMANCE OF A TWO-BLADE 10-FOOT-DIAMETER HELICOPTER ROTOR OPERATING AT TIP MACH NUMBERS UP TO 0.98, NASA TN D-245, April 1960.
24. Shivers, James P., HOVERING CHARACTERISTICS OF A ROTOR HAVING AN AIRFOIL SECTION DESIGNED FOR FLYING-CRANE TYPE OF HELICOPTER, NASA TN D-742, April 1961.
25. Shivers, James P., HIGH-TIP-SPEED STATIC-THRUST TESTS OF A ROTOR HAVING NACA 63⁽²¹⁵⁾ A018 AIRFOIL SECTIONS WITH AND WITHOUT VORTEX GENERATORS INSTALLED, NASA TN D-376, May 1960.
26. Gessov, Alfred, EQUATIONS AND PROCEDURES FOR NUMERICALLY CALCULATING THE AERODYNAMIC CHARACTERISTICS OF LIFTING ROTORS, NACA TN 3747, October 1956.
27. Gessov, Alfred, and Myers, Garry C., Jr., AERODYNAMICS OF THE HELICOPTER, New York, republished by Frederick Ungar Publishing Co., 1967.
28. Tanner, Watson H., CHARTS FOR ESTIMATING ROTARY WING PERFORMANCE IN HOVER AND AT HIGH FORWARD SPEEDS, United Aircraft Corporation, NASA CR-114, November 1964.
29. Tanner, Watson H., TABLES FOR ESTIMATING ROTARY WING PERFORMANCE AT HIGH FORWARD SPEEDS, United Aircraft Corporation, NASA CR-115, November 1964.
30. Bellinger, E. D., ANALYTICAL INVESTIGATION OF THE EFFECTS OF BLADE FLEXIBILITY, UNSTEADY AERODYNAMICS, AND VARIABLE INFLOW ON HELICOPTER ROTOR STALL CHARACTERISTICS, United Aircraft Research Laboratories, NASA CR-1769, September 1971.
31. Kisielowski, E., Bunstead, R., Fissell, P., and Chinsky, I., GENERALIZED ROTOR PERFORMANCE, Vertol Division, The Boeing Company; USAAVLABS Technical Report 66-83, U.S. Army Aviation Materiel Laboratories, Fort Eustis, Virginia, February 1967, AD 648 874.
32. Gessov, Alfred, and Crim, Almer D., A THEORETICAL ESTIMATE OF THE EFFECTS OF COMPRESSIBILITY ON THE PERFORMANCE OF A HELICOPTER ROTOR IN VARIOUS FLIGHT CONDITIONS, NACA TN 3798, October 1956.
33. Norman, David D., and Sultany, Dennis J., AN EMPIRICAL METHOD FOR CALCULATING THE POWER REQUIRED DUE TO COMPRESSIBILITY ON A SINGLE ROTOR HELICOPTER, Journal of the American Helicopter Society, Vol. 10, No. 3, July 1965, pp. 30-36.
34. Norman, David C., and Somsel, John R., DETERMINATION OF HELICOPTER ROTOR BLADE COMPRESSIBILITY EFFECTS - PREDICTION VS. FLIGHT TEST, Paper No. 105, presented at the American Helicopter Society 23rd Annual National Forum, May 1967.

35. Sultary, Dennis J., and Thomas, David W., DETERMINATION OF THE EFFECTS OF ROTOR BLADE COMPRESSIBILITY ON THE PERFORMANCE OF THE UH-1F, Flight Test Center Technical Report FTC-TR-65-17, Air Force Flight Test Center, Edwards Air Force Base, California, July 1965.
36. Somsel, John R., and Thomas, David W., DETERMINATION OF THE EFFECTS OF ROTOR BLADE COMPRESSIBILITY ON THE PERFORMANCE OF THE CH-47A HELICOPTER, Flight Test Center Technical Report, FTC-TR-66-46, Air Force Flight Test Center, Edwards Air Force Base, California, March 1967.
37. Barbini, Wayne J., and Heft, Edward L., DETERMINATION OF THE EFFECTS OF ROTOR BLADE COMPRESSIBILITY ON THE LEVEL FLIGHT PERFORMANCE OF THE CH-3C HELICOPTER, Flight Test Center Technical Report FTC-TR-67-10, Air Force Flight Test Center, Edwards Air Force Base, California, January 1967.
38. Parks, Dr. E. K., AN ANALYSIS OF HELICOPTER ROTOR BLADE COMPRESSIBILITY EFFECTS, Flight Research Branch Office Memo, Air Force Flight Test Center, Edwards Air Force Base, California, January 10, 1969.
39. Somsel, John R., DEVELOPMENT OF A DATA ANALYSIS TECHNIQUE FOR DETERMINING THE LEVEL FLIGHT PERFORMANCE OF A HELICOPTER ROTOR, Air Force Flight Test Center Technology Document No. 70-1, FTC-TD-70-1, Air Force Flight Test Center, Edwards Air Force Base, California, AD 703 719.
40. Vogeley, Arthur W., AXIAL MOMENTUM THEORY FOR PROPELLERS IN COMPRESSIBLE FLOW, NACA TN-2164, 1951.
41. Laitone, E. V., ACTUATOR DISK THEORY FOR COMPRESSIBLE FLOW AND SUBSONIC CORRECTION FOR PROPELLERS, Journal of Aeronautical Sciences, Vol. 20, No. 5, May 1953, pp. 365-6.
42. Delano, James B., and Crigler, John L., COMPRESSIBLE FLOW SOLUTIONS FOR THE ACTUATOR DISK, NACA RM L 53A07, March 1953.
43. Laitone, E. V., and Talbot, Lawrence, SUBSONIC COMPRESSIBILITY CORRECTIONS FOR PROPELLERS AND HELICOPTER ROTORS, Journal of Aeronautical Sciences, Vol. 20, No. 10, October 1953, pp. 683-690.
44. Head, R. M., THE EFFECT OF COMPRESSIBILITY ON THE THRUST AND POWER OF A HELICOPTER ROTOR, Douglas Aircraft Company Report No. SM-18475, August 1954, AD 106 710L.
45. Dingeldein, Richard C., CONSIDERATIONS OF METHODS OF IMPROVING HELICOPTER EFFICIENCY, NASA TN D-734, April 1961.
46. Prouty, R., TIP RELIEF FOR DRAC DIVERGENCE, Journal of the American Helicopter Society, Vol. 16, No. 4, October 1971, pp. 61-62.

47. Kuchemann, D., and Weber, J., THE SUBSONIC FLOW PAST SWEEP WINGS AT ZERO LIFT WITHOUT AND WITH BODY, Ministry of Supply, Aeronautical Research Council, Reports and Memoranda No. 2908, Her Majesty's Stationery Office, London, Great Britain, March 1953.
48. Lock, R. C., Powell, B. J., Sells, C. C. C. L., and Wilby, P. G., THE PREDICTION OF AEROFOIL PRESSURE DISTRIBUTIONS FOR SUB-CRITICAL VISCOUS FLOWS, AGARD Conference Proceedings No. 35, September 1968.
49. Spreiter, John R., AERODYNAMICS OF WINGS AND BODIES AT TRANSONIC SPEEDS, Journal of the Aero-Space Sciences, Vol. 26, No. 3, August 1959, pp. 465-486.
50. Anderson, Gordon F., and Carroll, J. B., EXPERIMENTAL INVESTIGATION OF ASPECT RATIO INFLUENCE AT HIGH SUBSONIC AND TRANSONIC SPEEDS, Brown University Technical Note WT-17: Air Research and Development Command, Office of Scientific Research, OSR TN 55-242, July 1955, AD 77 494.
51. Brebner, G. G., Wyatt, L. A., and Ilott, Gladys P., LOW SPEED WIND TUNNEL TESTS ON A SERIES OF RECTANGULAR WINGS OF VARYING ASPECT RATIO AND AEROFOIL SECTION, Aeronautical Research Council (Great Britain) Current Paper No. 916, October 1967.
52. Nelson, Warren H., and McDevitt, John R., THE TRANSONIC CHARACTERISTICS OF 22 RECTANGULAR, SYMMETRICAL WING MODELS OF VARYING ASPECT RATIO AND THICKNESS, NACA TN 3501, June 1955.
53. Sipe, O. E., Jr., and Gorenberg, N. B., EFFECT OF MACH NUMBER, REYNOLDS NUMBER AND THICKNESS RATIO ON THE AERODYNAMIC CHARACTERISTICS OF NACA 63A-SERIES AIRFOIL SECTIONS, Lockheed-California Company; USAAMI Technical Report 65-28, U.S. Army Aviation Materiel Laboratories, Fort Rucker, Virginia, June 1965, AD 619 153.

APPENDIX - COMPUTER PROGRAMS

The four computer programs discussed in this report are listed in the following pages. These programs are short and very straightforward. Thus a detailed description will not be given.

CORFAC

This program calculates the value of the right-hand side of equation (19).

Call Statement Variables

DUOU - the correction factor = value of equation (19)
TAU - thickness ratio
BETA - Prandtl-Glauert variable
MACH - Mach number
RBA - radial station as fraction of radius
RAD - radius in feet
CHD - chord divided by diameter

Switches

IFR - if equal to zero, does not print; if greater than zero, prints CORFAC variables
IFW - if equal to one, uses finite wing; if equal to zero, uses semi-infinite wing*
NTERM - if equal to three, uses three terms of the Taylor series**

TR

This subprogram calculates the drag coefficient CD using equations (20) through (23), the subroutine CORFAC, and an airfoil subroutine ERFOYL. Most of the variables pertain to ERFOYL and thus will not be described.

Switches

IMD - if equal to one, only Mach correction is calculated
IPRINT - if not equal to zero, then results at this point are printed.

TIPRLF

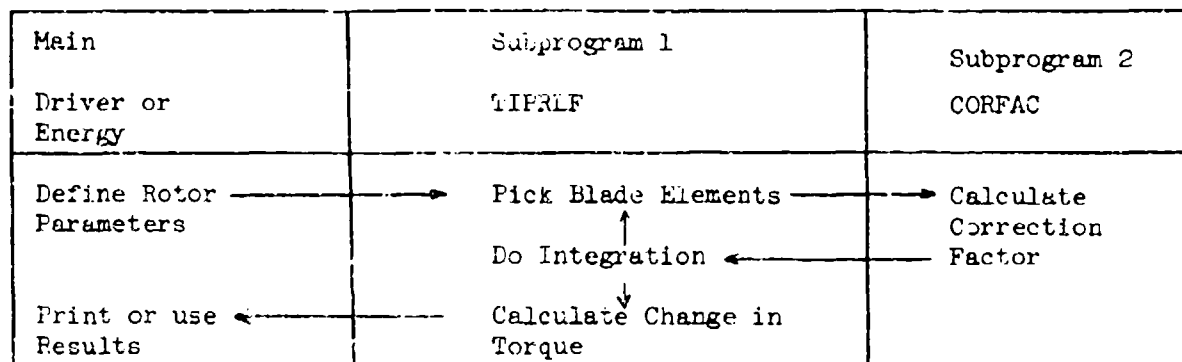
The subroutine TIPRLF, using CORFAC, generates a value of the change in torque coefficient per blade and the change in torque coefficient divided by solidity due to tip relief. CORFAC provides the tip relief correction factor while TIPRLF handles the integration process. The two subroutines are designed for final use with energy type programs. The integration uses the value of the correction factor at the mean of the interval, namely at

$$\frac{r_i + r_{i-1}}{2}$$

* As listed, IFW = 0

** As listed, NTERM = 3

Program-Subprogram Relationship



Identification:

Call TIPRLF (XMDA, OMGR, COSAL, VFPS, C1, XMU, NPSI, AC, DCQTR, RAD, CHD, TAU, SIGPB, BN, DCQTRS, NSTA, NRST, IPR)

COMMON

The values of the radial station to be used are in the COMMON statement.

Description:

The integration of a simplified blade element analysis for the tip relief correction is done using the mean value within the interval. Since the program is straightforward and not lengthy, only a few exceptions are described. The value of the integrand is calculated and summed along the radius before advancing to a new azimuth. If the advance ratio is less than 0.001, only one azimuthal station is calculated, and hover is assumed.

Warning Statements:

- a. If $M_{(1,90)}$ exceeds 0.995, the statement below is printed:
 ADVANCING TIP MACH NUMBER EXCEEDS ONE, $M_{(1,90)} = vx.yz$
- b. If the local Mach number at the first radial station exceeds the input value of the drag divergence Mach number, the following is printed:
 SPAR IS ABOVE DRAG DIVERGENCE MACH NUMBER

MNEMONICS LIST

Subroutine TIPRLF

<u>Program Symbol</u>	<u>Mathematical Model here</u>	<u>Explanation</u>
AC	a_c	Slope of compressible drag rise
BN	b	Number of blades
BETA	$\beta = \sqrt{1-M^2}$	Prandtl-Glauert factor
C1	a	Speed of sound
CHD	$c/2R$	Chord diameter ratio
COSAL	$\cos a$	Cosine rotor angle of attack
DCQTR	C_{QTR}	Change in torque coefficient for BN blades
DCQTRS	C_{QTR}/c	Change in torque coefficient divided by solidity for the BN blades
DELPSI	$\Delta\psi$	Step in azimuthal angle
DUOU	$\Delta U/U_\infty = \bar{G}_x$	Correction factor
GAM	$\Gamma = 1 + \frac{\gamma-1}{2} M^2$	Stagnation compressibility factor
IPR		Switch for detail printing
M190	$M_{1,90}$	Advancing tip Mach number, Note 1
ML	M	Local Mach number, Note 1
MLT	$M_{1,\psi}$	Tip Mach number at azimuth, Note 1
NFSI	$360/\Delta\psi$	Number of azimuthal stations
NRST		Largest number of radial stations used for the integration at any azimuth
NST		Total number of stations used for the integration
OMGR	ωR	Rotational tip speed in feet per second
PI	$= 3.1416$	
PSI	ψ	Azimuth angle, radians
R	\bar{r}	Radial station as fraction of radius

Note 1. These variables are declared as REAL.

Program Symbol	Mathematical Model Name	Explanation
RAD	R	Rotor radius
SIGPB	σ/b	Solidity per blade
SINPSI	$\sin \psi$	
SUM	Σ	Summation of integrand
TAU	τ	Airfoil thickness ratio
UL	$= \mu \sin \psi + \bar{r}$	Local normal velocity
VALUE		Integrand
VFPS	V	Forward speed
XMDA	M_{dd}	Drag divergence Mach number
XMU	μ	Advance ratio

TIP RELIEF CALCULATION DRIVER

This is a simple driver for TIPRLF written so that a particular rotor configuration is inputted and the tip relief torque coefficient is calculated at a series of advance ratios.

Input

The input data is put on three unformatted cards:

Card 1

RAD, BN, OMGR, CHD

Card 2

TAU, XMDA, C1, AC, COSAL

Card 3

LCASE, IPR, NPSI, LXMU, UXMU, DXMU, NRSET

The variables names on the first two cards are identical to those in TIPRLF.

<u>Variable Name</u>	<u>Explanation</u>	<u>Card</u>	<u>Position</u>
Rotor Characteristics:			
AC	slope of compressible drag rise	2	4
BN	number of blades	1	2
CHD	chord diameter ratio	1	4
COSAL	cosine of rotor angle of attack	2	5
C1	speed of sound	2	3
OMGR	rotational tip speed	1	3
RAD	radius	1	1
TAU	airfoil thickness ratio	2	1
XMDA	drag divergence Mach number	2	2
Program Switches			
XJMU (Declared Real)	lower	3	4
UXMU	upper	3	5
DXMU	step	3	6
LCASE	case number, negative for last case	3	1
IPR	detailed printing if positive	3	2
NPSI	number of azimuthal stations	3	3
NRSET	number (label) of set of radial stations	3	7

Restrictions

Up to three sets of radial stations may be used, each with up to 30 stations.

COMMON

The values of the set of radial stations to be used (determined by NRSET) are transferred by the COMMON.

Block Data:

The values of the three sets of radial stations are entered through block data statements.

Output

All output variables, except with detail print, are labeled. First all rotor characteristic variables are printed. Then a tabulation of μ , v , $M_{1,90}$, C_{QTR} , C_{QTR}/σ is given. The radial stations used are printed below the table.

Note:

After a tip Mach number of one is reached, only two more values of the advance ratios are used for calculations before going to the next set of inputs.

LISTING OF THE SUBROUTINE CORFAC

```

SUBROUTINE CORFAC (DUUU,TAU,BETA,MACH,RBA,RAD,CHD,IPR)
C
C THIS VERSION DIFFERS IN COMMON AND CALL STATEMENTS
C VALUES OF C1 ARE ENTERED AS DATA
REAL MACH
DATA C1,C2,C3/ -1.333,-0.80,-0.571/
FNB(U) = SQRT ( ( U*U ) + 1.)
FND(U) = 1.-SQRT((1./U)**2)/(1.+(1./U)**2))
FNE(U) = ((-6.*(U**4)) - (5.*U*U) - 2.) / ((FNB(U))**5)
FNF(U) = ((120.*(U**8))+(120.*(U**6))+(189.*(U**4))+(108.*(U**2))+14.)
NTERM = 3
PI = 3.1416
IF (MACH.GT.0.995) MACH = 0.995
BETA = SQRT ( 1. - (MACH*MACH))
SIGPH = CHD * (2./PI)
AR = 1./(PI*SIGPH)
CAR = BETA * AR
IF (RBA.LI.0.999) GO TO 40
G1 = 2.0
G2 = 0.00007
G3 = 0.40
GO TO 31
40 CONTINUE
Y = 1.-RBA
C
C NEAR COMPLEMENTARY WING
C
U = 1. / (Y*CAR * 2.)
UP = 1./U
G1 = +2.*FND(U)
IF (NTERM.NE.3) GO TO 10
G2 = (2.*FNE(U)+4.)/A.
G3 = (48.-(2.*FNF(U)/(FNB(U)**9)))/120.
10 CONTINUE
C
C FAR COMPLEMENTARY WING
C
31 CONTINUE
IFW = 1
IFW = 0
IF (IFW.NE.1) GO TO 30
U = 1. / (RBA*CAR*2.)
G1 = +2.*FND(U) + G1
IF (NTERM.NE.3) GO TO 30
G2 = (2.*FNE(U)+4.)/A. + G2
G3 = (48.-(2.*FNF(U)/(FNB(U)**9)))/120. + G3
11 CONTINUE
30 CONTINUE
DUUU = C1 * TAU * G1
IF (NTERM.EQ.3) DUUU = DUUU + (C2*TAU*G2) + (C3 * TAU * G3)
DUUU = DUUU / ( 4.*PI*BETA)
IF (IPR.GT.0) WRITE (3,300) Y,CAR,G1,G2,G3,DUUU,UP,U
300 FORMAT (1H,2F8.3,6(1X,E11.4))

```


LISTING OF THE SUBROUTINE TIPRLF

```

SUBROUTINE TIPRLF (XMDA,OMGH,COSAL,VFPS,C1,XMU,NPSI,AC,DCUTH
A ,RAD,CMD,TAU,SIGPB,NN,DCUTB,NSTA,NRST,IPR)
C IF IPR IS POSITIVE, THEN DETAIL PRINT
COMMON R(30)
REAL MLT,ML,M190
PI = 3.1416
DELPSI = 2.*PI/NPSI
SUM = 0.0
PSI = 0.0
NSTA = 0
NRST = 0
M190 = (OMGH + (VFPS+COSAL))/C1
IF (M190.GT.0.995) WRITE (3,304) M190
304 FORMAT (1H,'ADVANCING TIP MACH NUMBER EXCEEDS ONE,M(1,90)='F6.3)
200 CONTINUE
SINPSI = SIN(PSI)
MLT = (OMGH+VFPS+COSAL+SINPSI)/C1
IF (MLT.LT.XMDA) GO TO 202
NRS = 0
DO 201 I=1,30,1
IF (R(I).EQ.0.0) GO TO 202
C
RAV = (R(I) + R(I-1))/2.
C
ML = MLT + RAV
IF (ML.LT.XMDA) GO TO 201
NRS = NRS + 1
IF (I.EQ.1) WRITE (3,305)
305 FORMAT (1H,' SPAR IS ABOVE DRAG DIVERGENCE MACH NO')
IF (ML.GT.0.995) ML=0.995
UL = XMU * SINPSI + RAV
GAM = 1. + (0.2*ML*ML)
CALL CORFAC (DUOU,TAU,BETA,ML,RAV ,RAD,CMD,IPR)
VALUE = UL*UL*GAM*DUOU*R(I)*ML*(1./(BETA**2))
NSTA = NSTA + 1
DELR = R(I) - R(I-1)
SUM = SUM + (VALUE *DELPSI*DELR)
IF (IPR.GT.0) WRITE (3,300) PSI,R(I),ML,RAV ,VALUE,SUM
300 FORMAT (F15.0,F12.0,F0.3,3(4X,E15.7))
IF (R(I).EQ.1.0) GO TO 202
201 CONTINUE
202 CONTINUE
IF (XMU.GT.0.001) GO TO 214
PSIN = NPSI
SUM = SUM + PSIN
PSI = 6.281
214 CONTINUE
PSI = PSI + DELPSI
IF (NRS.GT.NRST) NRST = NRS
IF (PSI.LT.6.28) GO TO 200
DCQTR = SIGPB*BN + AC*SUM * (1./(4.*PI))
DCQTRB = DCQTR / (SIGPB*BN)
RETURN
END

```

C TIP RELIEF CALCULATION DRIVER

C

DIMENSION RR(3,30)

COMMON R(30)

REAL M190, LXMU

C IF IPR IS POSITIVE, THEN DETAIL PRINT

100 FORMAT (4F)

101 FORMAT (5F)

102 FORMAT (3I,3F,1)

103 FORMAT (4F,2I)

152 FORMAT (1M-)

160 FORMAT (1M,1X,F5.3,3X,F8.1,3X,F10.5,2(3X,E15.0),1X,13,4X,15)

161 FORMAT (1M-,1X,3MXMU,7X,4MVFPS,8X,7MM(1.92),6X,5HOCOTR,12X,

A 11MDELCO/SIGMA,5X,4HNSIA,3X,5HNRSTA)

100 FORMAT (1M1,1X,'LCASE IPR NPS1')

101 FORMAT (1M0,1X,'RADIUS BLADES OMEGAR SIG/BLADE SIGMA CHORD/Z
Z1A')

102 FORMAT (1M0,2X,'TAU MDRAGDIV AIRFOIL SLOPE SOUNDSPEED COSAL')

190 FORMAT (1M,1X,13,3X,12,2X,12)

191 FORMAT (1M,1X,F6.1,1X,F4.1,2X,F6.1,2(2X,F8.0),2X,F7.4)

192 FORMAT (1M,F5.3,2X,F5.2,6X,F8.4,4X,F7.1,6X,F9.6)

C

DATA (RR(1,1),101,30)/0.2,0.4,0.6,0.8,0.9,0.95,0.97,0.98,0.99,

A 0.995,1.0,1.000,0.0/

DATA (RR(2,1),101,30)/0.60,0.75,0.80,0.84,0.87,0.89,0.91,0.930,

A 0.940,0.950,0.9550,0.9600,0.9650,0.9700,0.9725,

B 0.9750,0.9800,0.9825,0.9850,0.9875,0.9890,0.9925,0.9920,

C 0.9935,0.9950,0.9960,0.9970,0.9980,0.9990,1.2/

DATA (RR(3,1),101,30)/0.7,0.75,0.8,0.85,0.875,0.9,0.925,

A 0.950,0.960,0.970,0.975,0.980,0.985,0.990,0.995,1.2,14.07/

PI = 3.1416

1 CONTINUE

READ (2,100) RAD, BN, OMGR, CHD

READ (2,101) TAU, XMUA, C1, AC, COSAL

READ (2,102) LCASE, IPR, NPS1, LXMU, DXMU, NXMU, NRSET

WRITE (3,100)

WRITE (3,101) LCASE, IPR, NPS1

SIGPB = CHD * (2./PI)

SIG = SIGPB * BN

XMU = LXMU

UMACH = 1.00 * (1.99 * OMGR * DXMU / C1)

WRITE (3,101)

WRITE (3,101) RAD, BN, OMGR, SIGPB, SIG, CHD

WRITE (3,102)

WRITE (3,102) TAU, XMUA, AC, C1, COSAL

WRITE (3,152)

IF (IPR,LT,0) WRITE (3,161)

DO 202 I=1,30

202 R(I) = RR(NRSET,I)

C

200 CONTINUE

VFPS = XMU * OMGR / COSAL

M190 = (OMGR * (VFPS * COSAL)) / C1

```
CALL T1PRLF (XMDA,OMGR,COSAL,VFPS,C1,XMU,NPST,AC,DCQTR,WAD,CMO,  
A TAU,SIGPR,BN,DCQTRS,NSTA,NRST,IPR)
```

C

```
IF (IPR.GT.0) WRITE (3,152)
```

```
IF (IPR.GT.0) WRITE (3,161)
```

```
WRITE (3,160) XMU,VFPS,M192,DCQTR ,DCQTRS,NSTA,NRST
```

C

```
XMU = XMU + DXMU
```

```
IF (XMU.GT.UXMI) GO TO 271
```

```
IF (M192.GT.UMACH) GO TO 281
```

```
GO TO 200
```

```
201 CONTINUE
```

```
WRITE (3,152)
```

```
DO 203 I=1,16,15
```

```
III = II * 14
```

```
203 WRITE (3,170) (R(I),I=1,III)
```

```
170 FORMAT (1H ,15F7.4)
```

```
IF (LCASE.GT.0) GO TO 1
```

```
STOP
```

```
END
```

AD-775 857



DEPARTMENT OF THE ARMY
US ARMY AIR MOBILITY RESEARCH & DEVELOPMENT LABORATORY
EUSTIS DIRECTORATE
FORT EUSTIS, VIRGINIA 23604

ERRATUM

USAAMRDL Technical Report 73-71

TITLE: Inclusion of Tip Relief in the Prediction of Compressibility
Effects on Helicopter Rotor Performance

Change the equation in the computer subroutine TR on page 48 from

$DELDC = - ((2. - MACH) / B1) * DELMM$

to

$DELDC = - ((2. - MACH * * 2) / B1) * DELMM$

REPRODUCED BY
NATIONAL TECHNICAL
INFORMATION SERVICE
U. S. DEPARTMENT OF COMMERCE
SPRINGFIELD, VA. 22161

